Bifurcation structures for multi-modal maps

Kai T. Hansen
Physics Department, University of Oslo,
Box 1048, Blindern, N-0316 Oslo, Norway.
e-mail: k.t.hansen@fys.uio.no

November 3, 1995

Abstract

We discuss the bifurcation structure in multimodal maps and construct explicitly the bifurcation diagrams for short periodic orbits in few-modal maps using symbolic dynamics. We conjecture this topological picture to be valid for all n-modal maps and perform numerical experiments for polynomial maps which agrees with the symbolic dynamics results.

In this article we will discuss the structure of bifurcations in the parameter space for n-modal maps of the interval. We want to show that an n-modal map has a universal global bifurcation structure for all periodic and non-periodic orbits in an n dimensional parameter space and explicit construct this parameter space. We discuss in detail the bifurcations of short periodic orbits in the maps of modality 4 or less, and discuss also the generic bifurcations for an n-modal map.

We define an n-modal map to be the map $\mathbb{R} \mapsto \mathbb{R}$;

$$x \mapsto f(x;\vec{a}) \tag{1}$$

where the function $f(x,\vec{a})$ is continuous in x and has n alternating minimum and maximum points at the values $x_{c_1} < x_{c_2} < \cdots < x_{c_n}$ which we denote the critical points of the map. The values of $\vec{a} = a_1, a_2, a_3, \ldots$ are the parameters of the map which we for convenience call $a, b, c, \ldots$, and we will write $f(x)$ as a shorthand notation for $f(x,\vec{a})$.

We let a string of signs denotes the increasing and decreasing intervals of $f(x)$; the string $+-+-\cdots$ denotes the map with the function $f(x)$ increasing for $x < x_{c_1}$, decreasing for $x_{c_1} < x < x_{c_2}$, etc., and $-+-+\cdots$ denotes the map with $f(x)$ decreasing for $x < x_{c_1}$, increasing for $x_{c_1} < x < x_{c_2}$, etc. If $f(x)$ is differentiable then the signs in the string are the signs of $f'(x)$ as x goes from $-\infty$ to ∞. We denote an n-modal map with a sign string a *signed n-modal map.*

If $f^{(m)}(x) - x$ for an n-modal map has more than $(n+1)^m - 1$ extremal points for some integer m, then is it possible with other bifurcations than those discussed here. The bifurcations which can take place if this is true are rather simple and are discussed in the end of this article. The simplest of these bifurcations is of importance when we discuss the bifurcations for an n-modal map bifurcating into an $n-2$-modal map as discussed below. For a unimodal map is a negative Schwarzian a sufficient but not necessary condition for the universal bifurcation structure. In the numerical examples of smooth maps we choose $f(x)$ as a polynomial, and when $f(x)$ is a polynomial of degree $n+1$ the map (1) has modality n or less.

The main results we obtain are the following;

Conjecture 1 *A periodic or non-periodic orbit in an n-modal map has bifurcations of codimension n or less.*

Conjecture 2 *The global topological structure of the bifurcation of all orbits in a signed n-modal map is universal and can be described in the symbolic dynamics parameter space $\kappa_1 \cdots \kappa_n$.*

In the following sections we show how this description works for unimodal, bimodal, trimodal and four-modal maps. In the last section we sketch a generic argument for the conjectures.

A useful observation is also

Proposition 1 *Odd n-modal maps $f(x,\vec{a})$, $n \in \{1,3,5,\ldots\}$, have the same bifurcation structure for the map $+-\cdots+-$ as for the map $-+\cdots-+$.*

This proposition follows from observing that mapping the function $f(x)$ into $g(x) = -f(-x)$ preserves all orbits with reversed sign; $g^{(t)}(x) = -f^{(t)}(-x)$, and changes the function f: $+-\cdots+-$ into the reversed function g : $-+\cdots-+$ if f has an odd number of critical points. If f has an even number of critical points both f and g have the structure $+-\cdots-+$ or both have the structure $-+\cdots+-$.

1 Symbolic Dynamics

We will, before discussing the examples, introduce the notation of the symbolic description of the map. Symbolic dynamics has been applied by Sarkovskii [19], Smale[20], Metropolis-Stein-Stein (MSS) [14], Milnor and Thurston[16] and others to study chaotic maps.

Following ideas Milnor and Thurston [16] we define symbols $s_t \in \{0,1,\ldots,n\}$ for a n-modal map with critical points $x_{c_1} < x_{c_2} < \cdots < x_{c_n}$

$$s_t = \begin{cases} 0 & \text{if} \quad x_t < x_{c_1} \\ i & \text{if} \quad x_{c_i} \le x_t < x_{c_{(i+1)}} \\ n & \text{if} \quad x_t \ge x_{c_n} \end{cases} \tag{2}$$

A bi-infinite symbol string $\cdots s_{-1}s_0s_1\cdots$ cannot be realized by more than one unstable bounded orbit in the n-modal map. A common notation is to let a line over a finite symbol string imply an infinite repetition of the string $\overline{s_1s_2\cdots s_m} = (s_1s_2\cdots s_m)^\infty$ and we adapt this notation here.

The important observation is that for $x' > x$ we get $f(x') > f(x)$ if $df/dx > 0$ and $f(x') < f(x)$ if $df/dx < 0$ for $f(x)$ differentiable, and for $f(x)$ not differentiable: $x' > x$ gives $f(x') \ge f(x)$ for $f(x)$ increasing and $f(x') \le f(x)$ for $f(x)$ decreasing. By turning the symbol s_t into $n - s_t$ when $df^{(t)}(x_0)/dx < 0$ (that is $f^{(t)}(x)$ decreasing at $x = x_0$) we obtain symbol strings that are ordered the same way as the space x. We call the new symbols; *well ordered symbols* $w_t \in \{0,1,\ldots,n\}$. For a map $+-\cdots$ we get the algorithm

$$\begin{aligned} w_1 &= s_1 \\ p_1 &= \begin{cases} 1 & \text{if} \quad s_1 \quad \text{even} \\ -1 & \text{if} \quad s_1 \quad \text{odd} \end{cases} \\ w_t &= \begin{cases} s_t & \text{if} \quad p_{t-1} = 1 \\ (n - s_t) & \text{if} \quad p_{t-1} = -1 \end{cases} \\ p_t &= \begin{cases} p_{t-1} & \text{if} \quad s_t \quad \text{even} \\ -p_{t-1} & \text{if} \quad s_t \quad \text{odd} \end{cases} \end{aligned} \tag{3}$$

and for the map $-+\cdots$

$$\begin{aligned} w_1 &= s_1 \\ p_1 &= \begin{cases} -1 & \text{if} \quad s_1 \quad \text{even} \\ 1 & \text{if} \quad s_1 \quad \text{odd} \end{cases} \\ w_t &= \begin{cases} s_t & \text{if} \quad p_{t-1} = 1 \\ (n - s_t) & \text{if} \quad p_{t-1} = -1 \end{cases} \\ p_t &= \begin{cases} -p_{t-1} & \text{if} \quad s_t \quad \text{even} \\ p_{t-1} & \text{if} \quad s_t \quad \text{odd} \end{cases} \end{aligned} \tag{4}$$

From these symbols we define a symbolic value $\tau \in (0,1)$ as the binary real number [2]

$$\tau = 0.w_1w_2w_3\ldots = \sum_{t=1}^{\infty} \frac{w_t}{(n+1)^t} \tag{5}$$

This symbolic value is useful because of the following property: assume $x_0' > x_0$ and the two symbol strings S' and S are given by the iterated of these two starting points; $x_1', x_2', x_3' \ldots$ and $x_1, x_2, x_3 \ldots$, then we will have $\tau' > \tau$.

We denote the symbol string obtained for $x_0 = x_{c_i}$ a ***kneading sequence*** K_i [14] and the symbolic value of this the ***kneading value***

$$\kappa_i = \tau(x_0 = x_{c_i}). \tag{6}$$

The n critical points $x_{c_1}, x_{c_2}, \ldots, x_{c_n}$ yield n different kneading sequences $K_1, K_2, \ldots, K_n$, and n kneading values $\kappa_1, \kappa_2, \ldots, \kappa_n$. The critical points yield the bound of the $f(x_t)$ values in an orbit given by the symbol s_t; the value of the i-th critical point $f(x_{c_i})$ restricts the value $f(x)$ can take on the interval $x_{c_{(i-1)}} < x < x_{c_{(i+1)}}$. For a point x between two critical points, the value $f(x)$ is smaller than the closest maximum point and larger than the closest minimum point.

To discuss the existence of an orbit given by a bi-infinite symbolic string $S = \ldots s_{-1} s_0 s_1 \ldots$ we have to define the extremum values of this symbol string: Let σ^k be an operator on S picking out the one side infinite symbolic string $s_{k+1} s_{k+2} s_{k+3} \ldots$, $k = \in \{\ldots, -1, 0, 1, \ldots\}$. The supremum values $\tau_i^{\max}$ are given as

$$\tau_i^{\max}(S) = \sup_k \tau_i(\sigma^k S) \tag{7}$$

and the infinitum values $\tau_i^{\min}(S)$

$$\tau_i^{\min}(S) = \inf_k \tau_i(\sigma^k S) \tag{8}$$

where the index i on τ restricts x_k to the appropriate interval such that the symbol s_k is either $s_k = i - 1$ or $s_k = i$.

The n admissibility conditions for the orbit S is

$$\begin{array}{rcl} \tau_i^{\max}(S) & \leq & \kappa_i \quad \text{for} \quad i \quad \text{odd for map} + - \cdots \text{ (even for map} - + \cdots) \\ \tau_i^{\min}(S) & \geq & \kappa_i \quad \text{for} \quad i \quad \text{even for map} + - \cdots \text{ (odd for map} - + \cdots) \end{array} \tag{9}$$

If $s_0 = 0$ there is no explicit minimum (maximum) restriction for the map $+ - \cdots$ $(- + \cdots)$, and if $s_0 = n$ there is no explicit maximum (minimum) restriction for the map $\cdots - +$ $(\cdots + -)$.

For odd-modal maps is a map $+ - \cdots + -$ mapped into the map $- + \cdots - +$ by the map $\kappa_i \rightarrow 1 - \kappa_i$ for all $i \in \{1, \ldots, n\}$, giving the same bifurcation structure, in agreement with proposition 1.

One complication is that as the parameters vary a map may lose some of the critical points and change modality. A maximum and a minimum point x_{c_i} and $x_{c_{(i+1)}}$ may merge, reducing the number of critical points in $f(x)$ to $(n-2)$ and giving a $(n-2)$-modal map. The symbols $s \in \{i-1, i, i+1\}$ are then indistinguishable and a symbol $i-1$ can be changed to $i+1$ by smoothly changing parameters. This bifurcation implies that orbits change symbolic description without becoming stable. This problem should not be avoided by introducing restrictions on the parameters of the function $f(x, \vec{a})$, because this is closely related to the singularity bifurcations, and unavoidable in applications to two-dimensional horseshoe maps [10].

2 Unimodal map

The simplest map with chaotic dynamics is the unimodal map with one critical point x_c (for the unimodal map we will omit the index $i = 1$). The bifurcation structure of the unimodal map has been much studied the last decades and the bifurcations of periodic orbits in this map are discussed in every elementary book on chaos. The period doubling route to chaos, scaling relations [7], and chaotic attractors are interesting structures in this map. The global ordering of orbits along a one-dimensional parameter line is described by using symbolic dynamics and is often denoted Sarkovskii ordering [19] or Metropolis-Stein-Stein (MSS) ordering [14]. One unimodal map is the polynomial of degree two

$$x \mapsto x^2 + c \tag{10}$$

with $x \in \mathbb{R}$ and the real parameter $c \in \mathbb{R}$ It has been proven by Milnor and Thurston [16] Sullivan and Douady and Hubbard[] that the number of orbits in this map is decreasing with the parameter c. Another equivalent and common parameterization of this quadratic map is

$$x \mapsto ax(x-1) \tag{11}$$

and a simple piecewise linear unimodal map is the tent map

$$x \mapsto \begin{cases} ax & \text{if} \quad x \leq 1/2 \\ a(x-1) & \text{if} \quad x > 1/2 \end{cases} \tag{12}$$

It follows from proposition 1 that the unimodal map $-+$ has the same bifurcation scenario as the map $+-$.

The ordering of orbits in a unimodal map can be described elegantly using the symbolic dynamics parameter κ. The orbit S is admissible for the $+-$ unimodal map when

$$\tau^{\max}(S) < \kappa \tag{13}$$

The value κ is increasing as a function of the parameter a in (11) in a staircase like way and we denote κ the symbolic dynamics parameter of the map. We then have that the orbit S exists in the parameter interval

$$\kappa \in [\tau^{\max}(S), 1] \tag{14}$$

A stable periodic orbit change symbolic description when one point in the orbit passes the critical point x_c (the superstable orbit), and the critical point is attracted to a stable orbit. The symbolic parameter κ jumps when the parameter a changes such that a stable orbit passes the superstable point, but is then constant from this point through the period doubling to the next superstable point. The jump in κ can be identified with a window on the parameter line a. This identification is specially useful in higher modal maps where it is much simpler to find the bifurcation structures in the k space than in the a parameter space.

Periodic orbits may bifurcate either as a pitchfork bifurcation if the orbit is created at a period doubling bifurcation point, or the orbit may be created at a tangent bifurcation. Non-periodic orbits are either born at a tangent bifurcation or at an accumulation point of a period doubling scenario.

Table 1 gives the symbol strings and the value $\tau^{\max}(S)$ for the short periodic orbits in the $+-$ unimodal map. The values $\tau^{\max}(S)$ in the table give the bifurcation points along the κ-parameter axis.

The non-periodic orbits are also created at a codimension 1 bifurcation which can be described in κ. The main difference from the periodic orbit bifurcation is that there is a large number of both homoclinic, hetroclinic and other non-periodic orbits with the same $\tau^{\max}$ value and therefore created at one parameter value. The topological entropy will increase at such a bifurcation.

In the unimodal map all orbits have a codimension 1 bifurcation and the global ordering of the bifurcations along a parameter axis is universal and can be expressed by a symbolic dynamics parameter axis. We may use the term *global codimension 1* for this system. A dynamical system has the global codimension 1 if all bifurcations have codimension 1 and there is a universal global ordering of the bifurcations. One natural universal parameter giving this ordering is the symbolic parameter κ.

The tent map (12) has the same ordering of orbits as the smooth map, but there are many orbits bifurcating at the same parameter value. These degenerated bifurcations may however be splitted up by modifying the map, changing it from the two piece linear map to something more complicated so these degenerated bifurcations are not universal.

We find it natural to call the tent map bifurcations; codimension 1 bifurcations. This will demand an extension of the definition of the term codimension. Instead of finding the number of derivatives which equal zero at the bifurcation point, and relate the equation to a normal form [8], we have to count the number of independent extremum points of the function $f^{(m)}(x) - x$ which approaches each other at the bifurcation point. In the case of smooth maps this must equals the ordinary definition.

It is of course not true that any parameterization of a unimodal map yields a monotone increase of the number of orbits. Choosing for example a new parameter $b = 1/\arcsin(4-a)$ in eq. (11) yields an infinite number of creation and destruction of orbits at $b = 0$, but this will always come from a non-monotone map from the chosen parameter into the κ symbolic parameter line.

3 Bimodal map

Bifurcation of the periodic orbits in the bimodal map is studied by many authors [1, 11, 12, 13, 15] and in addition to structures familiar from the unimodal map, it has the characteristic swallow tail signature and cusp singularities in a two dimensional parameter space. This is obtained because one orbit simultaneously may have two points in the neighborhood of the two critical points or the two critical points may merge together yielding a codimension 2 bifurcation.

The bimodal map has the two forms $+-+$ and $-+-$ drawn in Fig 1, with different bifurcation structures [15]. The smooth maps that we use for numerical calculations here is the polynomial map

$$x \mapsto f(x; a, b) = \pm x^3 - bx + a \tag{15}$$

The $+$ sign yields the $+-+$ map and the $-$ sign yields the $-+-$ map. Both maps have only bifurcation singularities with codimension 1 or 2 and the global ordering is given by two different 2-dimensional universal bifurcation planes. There are only two topological bifurcation planes for bimodal maps, one describing the bifurcations in the $+-+$ map and one describing the $-+-$ map. We will call these two the *global codimension 2 bifurcation planes* for $+-+$ or $-+-$.

The symbolic description of the orbits are given by eq. (2) with $n = 2$, and the three fixed points in Fig. 1 are denoted $\overline{0}$, $\overline{1}$ and $\overline{2}$.

The fixed points of a smooth map have a codimension 2 pitchfork bifurcation with a cusp at $a = 0$, $b = -1$ for the polynomial maps (15). The bifurcation curves are drawn in Fig. 2 (a) and (b). The singular point at the cusp is the parameter value where all three fixed points merge into one point illustrated in Fig. 2 (c) and (d). Away from this point in the parameter space may two fixed points merge at a tangent bifurcation. If the parameters changes such that the function $f(x)$ does not have any extremum points, the map is no longer bimodal but is a zero-modal map. The fixed point in the map $+-+$ is then unstable and can change symbolic dynamics from $\overline{0}$ to $\overline{2}$ by moving in a loop around the cusp in the parameter plane. The fixed point in the map $-+-$ is either stable or unstable and can also change symbolic dynamics description from $\overline{0}$ to $\overline{2}$. The possibility of changing symbolic description of an unstable periodic orbit is always related to the cusp structure of the codimension 2 bifurcation. For a function with a quadratic maximum/minimum ($f''(x_{c_i}) \neq 0$) we have a cusp where the width of the cusp increases as the distance to the cusp to the power 3/2 (here $\Delta a \sim (\Delta b)^{3/2}$).

The period doubling bifurcation of the fixed point in the $+-+$ map is a codimension 1 bifurcation along a smooth curve. The period 2 orbits in this map, $f^{(2)}(x) - x = 0$, have a codimension 2 bifurcation point. The bifurcation curves of the period 2 orbits are drawn in Fig.3 and this structure is called a swallowtail. The fixed point in the $-+-$ map bifurcates into two stable period 2 regions, each with a cusp shape similar to the fixed point in the $+-+$ map, Fig 2 (a).

All other periodic orbits in the bimodal maps has a swallowtail structure where they are stable.

In the symbolic parameter plane (κ_1, κ_2) the orbits exist in a rectangle. For the $+-+$ bimodal map an orbit S exists when

$$\begin{array}{rcccl} \tau_1^{\max}(S) & \leq & \kappa_1 & \leq & 1 \\ 0 & \leq & \kappa_2 & \leq & \tau_2^{\min}(S) \end{array} \tag{16}$$

and for the $-+-$ map

$$\begin{array}{rcccl} 0 & \leq & \kappa_1 & \leq & \tau_1^{\min}(S) \\ \tau_2^{\max}(S) & \leq & \kappa_2 & \leq & 1 \end{array} \tag{17}$$

Tables 2 and 3 gives the symbolic values for the bifurcation of the short periodic orbits for the bimodal maps $+-+$ and $-+-$.

Trying to get an overview of the bifurcations from reading the tables is difficult but drawing these bifurcation lines in the symbolic parameter space yields a clear and simple picture of the structures. In the Figs. 4 and 5 are the orbits for period 1 and 2, 3, and 4 drawn. To simplify the figures we have drawn three different figures for each map and the unaccessible k-values between the lines are shaded gray in Figs. 4 (a). This shows all the swallowtail structures in a topological correct way, and the existence and the relative position between the tails and the swallowtail crossings. Notice for example that the period 4 swallowtails have different positions with respect to each other in the $+-+$ and in the $-+-$ planes. This is also found numerically for the polynomial map.

Bifurcations of hetroclinic orbits in the (κ_1, κ_2) plane are discussed in ref.[9].

4 Trimodal map

The trimodal map $f(x)$ where the function f has three extremum points, yields a more complicated bifurcation structure than the bimodal map. Numerical investigations of periodic orbits for a trimodal polynomial map has been done by Mira et al[18], and they have drawn a number of bifurcation diagrams. This work shows that there is a rich structure of singularities in the parameter space. Further systematic investigations of the bifurcation structure of periodic and non-periodic orbits is so far not done. We show here that the symbolic dynamics parameter space describing a unimodal or bimodal map is simple to generalize, and yields a global codimension three description universal for trimodal maps. The bifurcations take place at simple 2-dimensional planes in the 3-dimensional symbolic parameter space $(\kappa_1, \kappa_2, \kappa_3)$. The bifurcations in any trimodal map are uniquely mapped into the bifurcations in this symbolic parameter space.

From proposition 1 follows that the map $+-+-$ and $-+-+$ yields identical bifurcation diagrams and we will here only discuss the map $+-+-$.

One trimodal polynomial map is given using the function

$$f(x) = -x^4 + cx^3 - bx - a. \tag{18}$$

The polynomial map has a 3-d parameter space (a, b, c) and we will draw bifurcation diagrams in the plane (a, b) keeping c constant in the numerical comparison with the symbolic parameter space bifurcations.

The map (18) does not have three critical points for all parameter values (a, b, c) and is consequently not always trimodal. A minimum and a maximum point may merge, reducing the map to a unimodal map with a one-parameter bifurcation structure. For this map with a constant parameter c the critical point mergings are two lines of constant b value in the (a, b) plane. Close to this critical point bifurcation there will be bifurcations not described by the symbolic parameter space of the type we found for the fixed point in the bimodal $-+-$ map above (see also section 8). The number of symbols changes from four symbols when the map is trimodal to two symbols when it is unimodal.

The trimodal map $+-+-$ has three critical points, x_{c_1} (max), x_{c_2} (min), and x_{c_3} (max), and the symbolic dynamics s_t is obtained from eq. (2) with $n = 3$. The well ordered symbols and the symbolic values are obtained from eqs. (3) and (5). According to eq. (9) an orbit S is admissible if

$$\begin{array}{rcl} \tau_1^{\max}(S) & \leq & \kappa_1 \\ \tau_2^{\min}(S) & \geq & \kappa_2 \\ \tau_3^{\max}(S) & \leq & \kappa_3. \end{array} \tag{19}$$

The bifurcations of orbits are 2-dimensional planes in a 3-dimensional symbolic parameter space. The bifurcations planes are determined by calculating the three extremum values for orbit S and the numbers for the periodic orbits of length 1, 2 and 3 are given in table 4. These bifurcation planes are drawn in Figures 6, 7 and 8. The map is trimodal if $\kappa_1 > \kappa_2$ and $\kappa_3 > \kappa_2$ and the border planes $\kappa_1 = \kappa_2$ and $\kappa_3 = \kappa_2$ are also drawn in the figure; the trimodal bifurcations take

place inside the skew-pyramidal region. Crossing the planes $\kappa_1 = \kappa_2$ and $\kappa_3 = \kappa_2$ imply that one moves into a unimodal map where the bifurcation theory for unimodal maps described above is valid.

The interpretation of the figures 6, 7 and 8 may seem difficult the first time, but it is actually quite simple. One can read out from these figures the different tails with stable orbits, cusp structures and coexisting stable orbits. One may draw all bifurcation planes in the same figure but we have chosen to draw the period 2 and period 3 orbits in different figures to simplify the understanding. We have not drawn figures of period four or any longer cycles. This can be done in exactly the same way and demands only some patience as the structure becomes rather complicated. The bifurcation structure is described by these tables and figures and below we will compare this topological description with a numerical example. In interpreting the figures it may be helpful to notice that when $\kappa_3 = 1$ then the map is a bimodal $+-+$ map with one additional function segment such that the bifurcations are the bifurcations described above for this bimodal map with some new structures added. For $\kappa_1 = 1$ the map is a bimodal $-+-$ map with one addition segment, and we should obtain the bifurcations of this map together with some new structures.

We adapt as convention to describe bifurcations that $\overline{\{s_1, s_2, s_3\}}$ is the three fixed points $\overline{s_1}$, $\overline{s_2}$, and $\overline{s_3}$ in a cusp, $\overline{\{s_1, s_2\}\{s_3, s_4\}}$ is equivalent with the four period two orbits $\overline{s_1 s_3}$, $\overline{s_1 s_4}$, $\overline{s_2 s_3}$ $\overline{s_2 s_4}$ in a swallowtail, the notation $s_1\overline{\{s_2, s_3, s_4\}}$ is short for the three period two orbits $\overline{s_1 s_2}$, $\overline{s_1 s_3}$ and $\overline{s_1 s_4}$ in a cusp, etc.

4.1 Fixed points

In figure 6 the bifurcation diagram for the fixed points in $(\kappa_1, \kappa_2, \kappa_3)$ is drawn. The point $(1.0, 0.0, 1.0)$ corresponds to the complete trimodal repellor and is in figure 6 the corner closest to the viewer. The κ_2 axis is hidden behind the bifurcation planes. The figure is read as follows; at the horizontal plane marked 3 the fixed point with symbolic description $\overline{3}$ becomes super-stable and changes symbolic description to $\overline{2}$. When κ_3 decreases further, the two fixed points $\overline{2}$ disappear at the horizontal plane marked 2 in figure 6. The fixed point $\overline{1}$ disappears either at a plane with constant κ_1 or with constant κ_2. If we let κ_1 decrease, the fixed point $\overline{1}$ changes symbolic description to $\overline{0}$ and the two fixed points $\overline{0}$ disappear at $\kappa_1 = 0$. Another possibility is that we let κ_2 increase and then the fixed point $\overline{1}$ changes symbolic description to $\overline{2}$ and the two fixed points $\overline{2}$ disappear at the vertical plane marked 2 in figure 6.

If we try to follow a fixed point $\overline{3}$ while κ_1 decreases or κ_2 increases we can pass into the unimodal map regime through the plane $\kappa_1 = \kappa_2$, without any bifurcations of the fixed point. In figure 6 we see that it is possible to enter the trimodal region at the plane $\kappa_2 = \kappa_3$ where the fixed point $\overline{1}$ exists but not the fixed point $\overline{3}$. We may therefore change the symbolic description of the fixed point by smooth parameter changes without ever making the fixed point stable. Since the sign of the derivative cannot change, the fixed point $\overline{3}$ can change only into $\overline{1}$, and the fixed point $\overline{2}$ only into $\overline{0}$.

We can now read off which singularities we have and how these are connected in the $(\kappa_1, \kappa_2, \kappa_3)$ space. The bifurcation planes for the orbits $\overline{1}$ and $\overline{2}$ give both a corner on a plane which is a border of the transition to a unimodal map. Since $\overline{1}$ is a stable orbit the cusp $\overline{\{0, 1, 2\}}$ is of the same type as the $+-+$ fixed point, Fig. 2 (a), while $\overline{2}$ is an unstable orbit and the cusp $\overline{\{1, 2, 3\}}$ is of the same type as the $-+-$ fixed point, Fig. 2 (b). We find that the tail $\overline{\{1, 2\}}$ connects the two corners (cusps) in Fig. 6.

We now compare figure 6 with two scans of the parameter plane (a, b) with $c = -3$ and $c = 0$, figure 10 (a) and (b). These scans is topological equivalent to surfaces cutting through the symbolic parameter space of figure 6.

In the (a, b) plane in Fig. 10 (a) all regions with a stable fixed point are connected; and this is predicted in the picture of the topological parameter space. The two horizontal planes $\overline{3}$ and $\overline{2}$ are associated with one tail with a stable fixed point. As κ_2 increases in figure 6, this tail connects in the cusp to the tail associated with the planes for $\overline{2}$ and $\overline{1}$ with constant κ_2. Decreasing κ_1 in this tail gives the cusp transition to the tail associated with the region between the constant κ_1 plane

of $\overline{1}$ and the $\kappa_1 = 0$ line where $\overline{0}$ bifurcates. We see that this last region crosses the first region of the planes of $\overline{3}$ and $\overline{2}$, and this is also the case in the (a, b) plane in figure 10 (a).

In figure 10 (b) is $c = 0$ and we have a bifurcation plane which goes through the codimension 3 singularity where the map is $-x^4 + x$. The two cusps in figure 10 (a) move closer to each other as c decreases and they have merged into one point for $c = 0$ at $a = 0$, $b = -1$.

4.2 Period 2 orbits

Figure 7 shows the planes in the topological parameter plane where both the fixed points and the period 2 orbits bifurcate. This figure is interpreted in a similar way as figure 6.

We know from the bimodal map that period 2 orbits have a swallowtail crossing, and we do find swallowtails in figure 7. On the top plane, $\kappa_3 = 1$, we find the same swallowtail crossing as in the bimodal plane in figure 4 (a). The symbols of the orbits in this crossing are $\overline{\{1,2\}\{0,1\}}$ as in the bimodal case, and the structure is the same, only the scale is slightly changed since we here use base 3 to calculate κ_1 and κ_2. In figure 7 we find another swallowtail for $\kappa_2 = 0$ which includes the orbits $\overline{\{2,3\}\{0,1\}}$. The two swallowtail crosses are directly connected to each other by having the tail $\overline{2\{0,1\}}$ in common. The two cusps in the $-+-$bimodal map, Fig. 5 (a), we find here at the $\kappa_1 = 0$ plane, now with the labels $\overline{1\{1,2,3\}}$ and $\overline{3\{1,2,3\}}$. These exist on the $\kappa_2 = \kappa_3$ plane. There are also two new cusp singularities; $\overline{0\{1,2,3\}}$ on the $\kappa_2 = \kappa_3$ plane and $\overline{3\{0,1,2\}}$ on the $\kappa_1 = \kappa_2$ plane. Fig. 7 shows how these cusps and swallowtails are connected to each other with tails of stable orbits.

The scan of the parameter plane (a, b) with $c = -3$ in figure 11 (a) shows the two swallowtail crosses, the four cusp singularities, and the common tails. We find here all the bifurcations predicted by the topological description. Choosing a different parameter plane may give a cut through the structures where codimension two singularities have merged into codimension three singularities, or we may have less singularities. Figure 11 (b) shows the (a, b) plane for $c = -2.2$ where some of the structures have merged together.

4.3 Period 3 orbits

The period 3 orbits form a rather complicated structure in the trimodal parameter space, and without the topological parameter space bifurcation diagrams would it be difficult to have any overview of the bifurcations at all. In figure 8 all bifurcation planes corresponding to the values of $\tau_i^{\max}$ listed in table 4 are drawn. To simplify the reading, the diagram is also drawn in figure 9 with the labels restricted to the swallowtail crossings in the three planes $\kappa_1 = 1$, $\kappa_2 = 0$ and $\kappa_3 = 1$.

A general observation is that many period 3 orbits have all the bifurcation planes in the interior of the trimodal region. Out of 20 orbits there are 6 orbits that only have two τ_i values giving only two bifurcation planes of the box of existence, and there are 2 orbits which have three values of τ_i but with one corner outside the trimodal region. 6 orbits have the corner of the box of existence on the edge of the trimodal region giving six cusp bifurcation singularities. Hence 12 period 3 orbits cannot change the symbolic dynamics description without getting super-stable while we found that all the fixed points could change symbolic description adiabatically. For long orbits only a small fraction of all orbits can change symbols because for these orbits there are few symbol strings which do not have any symbols $(i-1)$ or (i) such that τ_i does not exist, or that $\tau_2^{\min}$ is larger than either $\tau_1^{\max}$ or $\tau_3^{\max}$. Most codimension two structures are therefore swallowtails and not cusps for long periodic orbits.

The plots in figure 12 show some scans of the parameter plane (a, b) for the map (18) where the period 3 orbits are stable. The swallowtail crosses are labeled as, and should be compared to, the topological swallowtail crosses in figure 9. In figure 9 there is a closed structure consisting of the six swallowtail crosses $\overline{2\{1,2\}\{0,1\}}$, $\overline{3\{1,2\}\{0,1\}}$, $\overline{\{2,3\}2\{0,1\}}$, $\overline{\{2,3\}1\{0,1\}}$, $\overline{\{2,3\}\{1,2\}0}$ and $\overline{\{2,3\}\{1,2\}1}$. These are connected by tails to each other but not to any other crosses, and they all bifurcates inside the bifurcation box of $\overline{122}$, strictly inside the trimodal region. All these orbits disappear before the map becomes unimodal. Figures 12 (a) and (b) show that increasing the parameter c yields a (a, b) plane corresponding to a surface cutting deeper in the topological

parameter space in figure 9. In figure 12 (b) the surface cuts down in the $(\kappa_1, \kappa_2, \kappa_3)$ plane where the swallowtails in the closed structure start to merge together. Increasing c further yields a surface below the box $\overline{122}$ and will remove all traces of this structure from the (a, b) plane.

In figure 12 (b) we have labeled the other three swallowtails and six cusp singularities which are connected to each other by tails as predicted by the topological picture in figure 8. The only structure leaving from this connected structure in the parameter plane is the tails that become the normal period 3 window in the unimodal map.

4.4 Homoclinic orbits

Bifurcations of homoclinic and heteroclinic orbits or other non-periodic orbits can also be described in the symbolic dynamics plane. Some of these bifurcations curves determine band merging bifurcations and other changes in the structure of the non-wandering set of orbits in the system.

The method is the same for determining these bifurcation curves in the symbolic parameter space using eqs. (7), (8), and (9). In the generic case $\tau_i^{\max}$ may be a limiting supremum value instead of a simple maximum value and correspondingly for $\tau_i^{\min}$. Here we just give one example of non-periodic orbits to illustrate the method and the difference between periodic and non-periodic orbits.

As an example we choose to look at the bifurcations of the six homoclinic orbits $S = \overline{1}\{1,2\}\{0,1\}\{2,3\}3\overline{1}$. There will be a codimension 3 singularity for the parameter values where $f(x_{c_2}) = x_{c_1}$, $f(x_{c_1}) = x_{c_3}$, and $f(x_{c_3})$ maps first to a point larger than x_{c_3} and then into the unstable fixed point with symbolic description $\overline{1}$. This parameter point is the merging point of bifurcation planes with constant κ_1, κ_2, and κ_3 values. We find the following bifurcation planes for the six orbits:

$$\begin{aligned}
&\tau_3^{\max}(S) = \tau_3(3\overline{1}) = .3\overline{21}\\
&\tau_1^{\max}(S) = \tau_1(23\overline{1}) = .23\overline{21}\\
&\tau_1^{\max}(S) = \tau_1(33\overline{1}) = .30\overline{12}\\
&\tau_2^{\max}(S) = \tau_2(023\overline{1}) = .023\overline{21}\\
&\tau_2^{\max}(S) = \tau_2(033\overline{1}) = .030\overline{12}\\
&\tau_2^{\max}(S) = \tau_2(133\overline{1}) = .103\overline{21}\\
&\tau_2^{\max}(S) = \tau_2(123\overline{1}) = .110\overline{12}
\end{aligned} \tag{20}$$

These planes give the bifurcations in the symbolic parameter plane and in Fig. 13 these bifurcation curves are drawn in the (a, b) parameter plane. We find the curves ordered according to the symbolic values and connected together in cusps as predicted by the symbolic dynamics. The codimension 2 cusps here are narrower than for periodic orbits ($\Delta a \sim (\Delta b)^2$ instead of $\Delta a \sim (\Delta b)^{3/2}$) as discussed in ref.[9].

5 Four-modal map

We also extend our discussion of bifurcations to the four-modal maps. The four-modal map yields a 4-dimensional parameter space and the bifurcation structures are difficult to draw even in the symbolic parameter space $(\kappa_1, \kappa_2, \kappa_3, \kappa_4)$. An orbit exists in a 4-dimensional cube in the the parameter space and the 3-dimensional borders of the periodic orbits of length 1, 2 and 3 in symbolic parameter values are given in tables 5, 6, 7, and 8. Even if the complete bifurcation diagram cannot be drawn directly, much information can be obtained by investigating these tables and from drawing the bifurcation lines in all the 2-dimensional subspaces (κ_i, κ_j) of the symbolic parameter space. One can then find the possible swallowtails and cusps and which tails that may connect the different structures. This yields the topological structure of the possible 2-dimensional parameter scans of a 4-dimensional parameter space. A 2-dimensional surface cannot surround a 4-dimensional object and a typical numerically obtained 2-dimensional parameter plane will not combine all the swallowtails and cusps described in the symbolic parameter space.

In Fig. 14 the six projections of the bifurcation curves for the fixed points and the period 2 orbits are drawn for the $+-+-+$ map. The corresponding bifurcation diagrams for the $-+-+-$ map are drawn in Fig. 15. The bifurcation lines are labeled and the tails and crossings are shaded

gray. The bifurcation curves where the four-modal map bifurcates into a bimodal map; $\kappa_1 = \kappa_2$, $\kappa_2 = \kappa_3$, and $\kappa_3 = \kappa_4$ are indicated by a dashed lines.

To find out which possible bifurcation structures this gives for a specific map we can combine the different tails with the same labeling from the different planes in Figs. 14 or 15. This yield the possible bifurcation structures. We find that there are different choices to combine the tails of period two orbits and one choice cannot connect once all codimension two singularities in a simple plane. To compare Figs. 14 and 15 with a numerical example we have chosen to investigate the polynomial map

$$f(x) = \pm x^5 + dx^4 + cx^3 - bx + a. \tag{21}$$

The + sign yields the $+-+-+$ map and the $-$ sign yields the $-+-+-$ map. Keeping two of the parameter constant we can scan the plane given by the two other parameters and draw the bifurcation curves.

Numerical scans finding stable fixed points in the (a, b) plane of the map (21) keeping d and c fixed are shown in Fig. 16 and revels the structures predicted by the topological picture. The bifurcation structure in Fig. 16 (a) is given by combining the cusps and tails in Fig. 14. The cusp $\overline{\{1,2,3\}}$ in Fig. 14 (d) has the unstable fixed point $\overline{2}$ as common orbit and the cusp is therefore of the same type as in the $-+-$ bimodal map, Fig. 5 (a) and 2 (b). The cusps $\overline{\{0,1,2\}}$ in Fig. 14 (a) and $\overline{\{2,3,4\}}$ in Fig. 14 (f) are of the type existing in the $+-+$ bimodal map. In Figs. 14 (b), (c), and (e) we can read off how the tails cross each other; in 14 (b) tail $\overline{\{0,1\}}$ crosses tail $\overline{\{2,3\}}$, in 14 (c) tail $\overline{\{0,1\}}$ crosses tail $\overline{\{3,4\}}$, and in 14 (e) tail $\overline{\{1,2\}}$ crosses tail $\overline{\{3,4\}}$. Exactly these three cusps and three crossings of stable tails are found in Fig. 16 (a). The bifurcation structure in Fig. 16 (b) is given combining the cusps and tails in Fig. 15 in a similar way.

The areas with stable period two orbits in the (a, b) plane for the $+-+-+$ map (21) are drawn in Fig. 17. The 5 swallowtail crossings and 4 of the 8 cusp bifurcations in Fig. 14 are combined according to the tails in Fig. 14. The remaining 4 cusp singularities in the $\kappa_1 = \kappa_2$ and $\kappa_3 = \kappa_4$ spaces are not present in this (a, b) plane.

Other combinations of swallowtails and cusps can be constructed which includes the cusps left out and will be obtainable in some other 2-dimensional scan of combinations of the parameters in eq. (21). In Fig. 18 have we scanned a part of the (d, a) plane and kept c and b fixed. In this plane two of the other cusps are present and combined with swallow tails according to a different choice in Fig. 14. The two cusps here are $\overline{3\{0,1,2\}}$ and $\overline{4\{0,1,2\}}$ from Fig. 14 (a) together with the two swallowtails $\overline{\{0,1\}\{3,4\}}$ from Fig. 14 (c) and $\overline{\{1,2\}\{3,4\}}$ from Fig. 14 (e).

Similar combinations of bifurcation structures can be obtained for the $-+-+-$ map. In Fig. 19 a scan of the (a, b) plane shows combinations of swallowtails and cusps in agreement with Fig. 15.

Similar topological pictures of the bifurcations of period 3 orbits can be drawn using the numbers given in tables 6 and 8.

6 Higher modal map

For n-modal maps with $n > 4$ we can construct topological parameter spaces in the same way, but the complexity of the bifurcation diagrams increases because the dimension of the parameter space increases and the number of orbits grows very fast. Two dimensional (κ_i, κ_j) planes yield the different codimension two singularities and the combination of these.

The fixed points in an n-modal map is connected with codimension 1 bands between the $n-1$ codimension 2 singularities where $\kappa_i = \kappa_{i+1}$ $n \in \{1, 2, \ldots, n-1\}$. These may merge into higher codimension singularities and if all merge together at the same parameter value the singularity has codimension n. The singularities of longer periodic orbits do also have codimension n or less.

7 Monotonicity

An interesting question is whether there exist paths in the parameter space along which orbits are only created and never destroyed. There are claims that this will always be the case in systems

more complicated than the unimodal map[4] but there has been arguments against this for the bimodal map[15]. In the n-modal maps discussed here is it clear that orbits are only created and never destroyed along any path where the symbolic parameters with even (odd) index decreases and with odd (even) index increases for the $+-+\cdots$ ($-+-\cdots$) map. From any point in the n dimensional $(\kappa_1,\ldots,\kappa_n)$ space which correspond to an n-modal map there is then a cone of dimension n which yields a monotone increment in the number of orbits and therefore a monotone change in the topological entropy. There do not exist a proof that e.g. the parameters in a polynomial map can be mapped into such a path, but it is highly unlikely that this is not possible.

A possible problem is that in a cusp, especially cusps for non-periodic orbits like in Fig. 13, the cone of parameters $\vec{a}$ which maps into the large cone of $\vec{\kappa}$ may be very narrow. This imply that there can be few paths with monotone behavior, but they may still exist. We will therefore conjecture that in any n-modal map there will exist a one-dimensional parameter curve through any parameter point where orbits are created in one direction and orbits destroyed in the other direction along this curve.

A similar argument can be made for the pruned Smale horseshoe maps[10] and in these maps homoclinic cusps are broader than in one dimensional map. An article presenting results for the Henon map is in preparation.

8 Bifurcations outside kneading theory

There may be bifurcations in a n-modal map not described by kneading theory if the function $f(x)$ has n extremum points but $f^{(m)}(x)-x$ has more than $(n+1)^m-1$ extremum points for some positive integer m. We can construct extreme examples like the map $f(x)=x+x^3\sin(1/x)+a$ for $0<x<1$ which do not have any extremal points in this interval but in the limit $a\to 0$ creates infinitely many stable and unstable fixed points because $f(x)-x=x^3\sin(1/x)+a$ has an infinite number of extremum points. Such bifurcations can however never give a chaotic attractor. The bifurcations only create a pair of one stable and one unstable orbit and it will not be any period doubling bifurcation creating further orbits.

The bifurcation of the fixed point in the bimodal $-+-$ map, Fig. 2 (d) behind the cusp is a bifurcation of this kind. The fixed point in the 0-modal map, $f'(x)<0$, becomes stable by creating an unstable period 2 orbit, but there are no further bifurcation of these orbits until $f(x)$ has become 3-modal.

The author thanks Predrag Cvitanović for valuable discussions and the Norwegian Research Council (NFR) and the Alexander von Humboldt foundation for financial support. The author is grateful for the hospitality at the Niels Bohr Institute, Copenhagen, Denmark and the Institute for Physics, University of Freiburg, Germany, where parts of this work was done.

References

[1] J. Belair and L. Glass, *Physica* **16 D**, 143 (1985).

[2] P. Cvitanović, G. H. Gunaratne, I. Procaccia, *Phys. Rev. A* **38**, 1503 (1988).

[3] S.P. Dawson, R. Galeeva, J. Milnor, and C. Tresser in B. Branner and P. Hjort ed., *Real and Complex Dynamical Systems*, 165-183 (Kluwer Academic Publishers, Dordrecht, 1995).

[4] S.P. Dawson, C. Grebogi, I. Kan, H. Koçak, and J.A. Yorke, *Phys. Lett. A*, **162**, 249 (1992). S.P. Dawson, C. Grebogi, and H. Koçak, *Phys. Rev. E* **48**, 1676 (1993).

[5] A. Douady in B. Branner and P. Hjort ed., *Real and Complex Dynamical Systems*, 65-87 (Kluwer Academic Publishers, Dordrecht, 1995).

[6] A. Douady and J. H. Hubbard, *Ann. Sci. Ec. Norm. Sup., Paris*, **18**, 287 (1985).

[7] M. J. Feigenbaum, *J. Stat. Phys.* **19**, 25 (1978); **21**, 669 (1979).

[8] M. Golubitsky and D.G. Schaeffer, *Singularities and groups in bifurcation theory,* Applied mathematical sciences **51**, (Springer, Berlin, 1985).

[9] K.T. Hansen, *Phys. Rev. E* **50**, 1653 (1994).

[10] K.T. Hansen, Ph.D. thesis, University of Oslo, Norway (1994).

[11] R.S. MacKay and C. Tresser, *Physica* **D 19**, 206 (1986).

[12] R.S. MacKay and C. Tresser, *Physica* **D 27**, 412 (1987).

[13] R.S. MacKay and J. B. J. van Zeijts, *Nonlinearity* **1**, 253 (1988).

[14] N. Metropolis, M.L. Stein and P.R. Stein, *J. Comb. Theo.* **A15**, 25 (1973).

[15] J. Milnor, *Experimental Math.*, **1**, 5 (1992).

[16] J. Milnor and W. Thurston, "On iterated maps of the interval", *Lec. Notes in Math.* **1342,** 465 (Springer, Berlin, 1988).

[17] C. Mira, *Chaotic Dynamics* (World Scientific, Singapore, 1987).

[18] C Mira, JP Carcassès, M Bosch, C Simó, and JC Tatjer, *Int. J. Bif. and Chaos* **1**, 339 (1991).

[19] A. N. Sarkovskii, *Ukranian Math. J.* **16**, 61 (1964).

[20] S. Smale, *Bull. Am. Math. Soc.* **73**, 747 (1967).

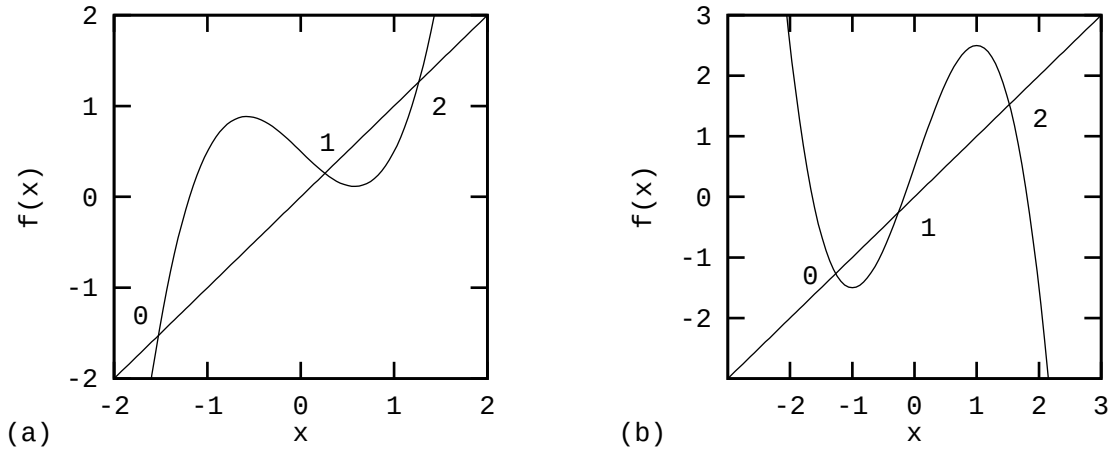

Figure 1: The bimodal functions $f(x)$ (a) $+-+$ and (b) $-+-$.

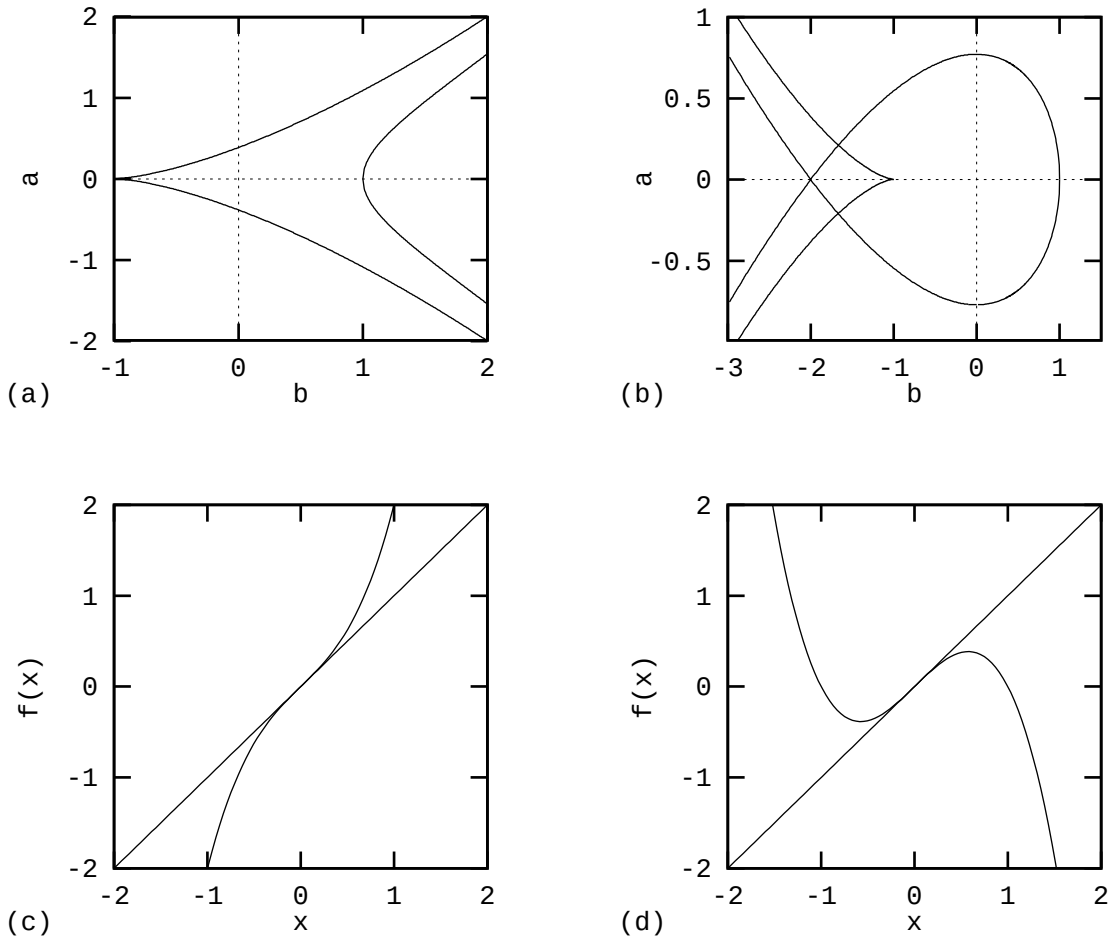

Figure 2: Codimension 2 bifurcation of the fixed points in the smooth bimodal maps (a) $+-+$ and (b) $-+-$. We have drawn the bifurcation curves in the parameter plane and the function $f(x)$ at the cusp point in (c) and (d).

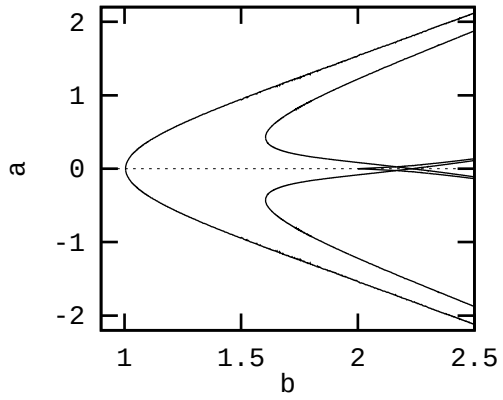

Figure 3: The bifurcation curves for the period 2 orbit in the $+-+$ map.

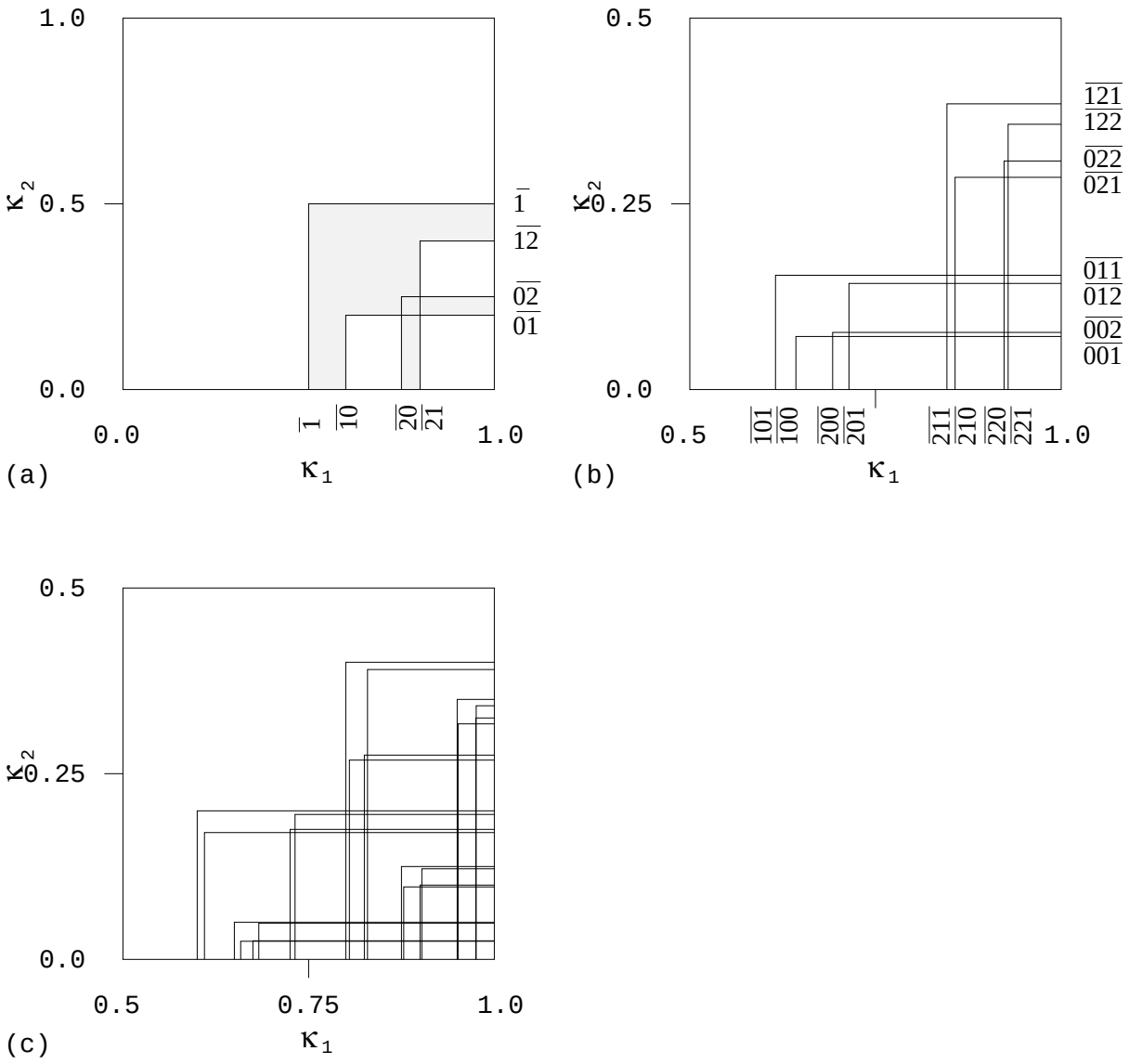

Figure 4: Symbolic parameter plane for the bimodal maps $+-+$ (a) period 1 and 2 orbits, (b) period 3 orbits, (c) period 4 orbits.

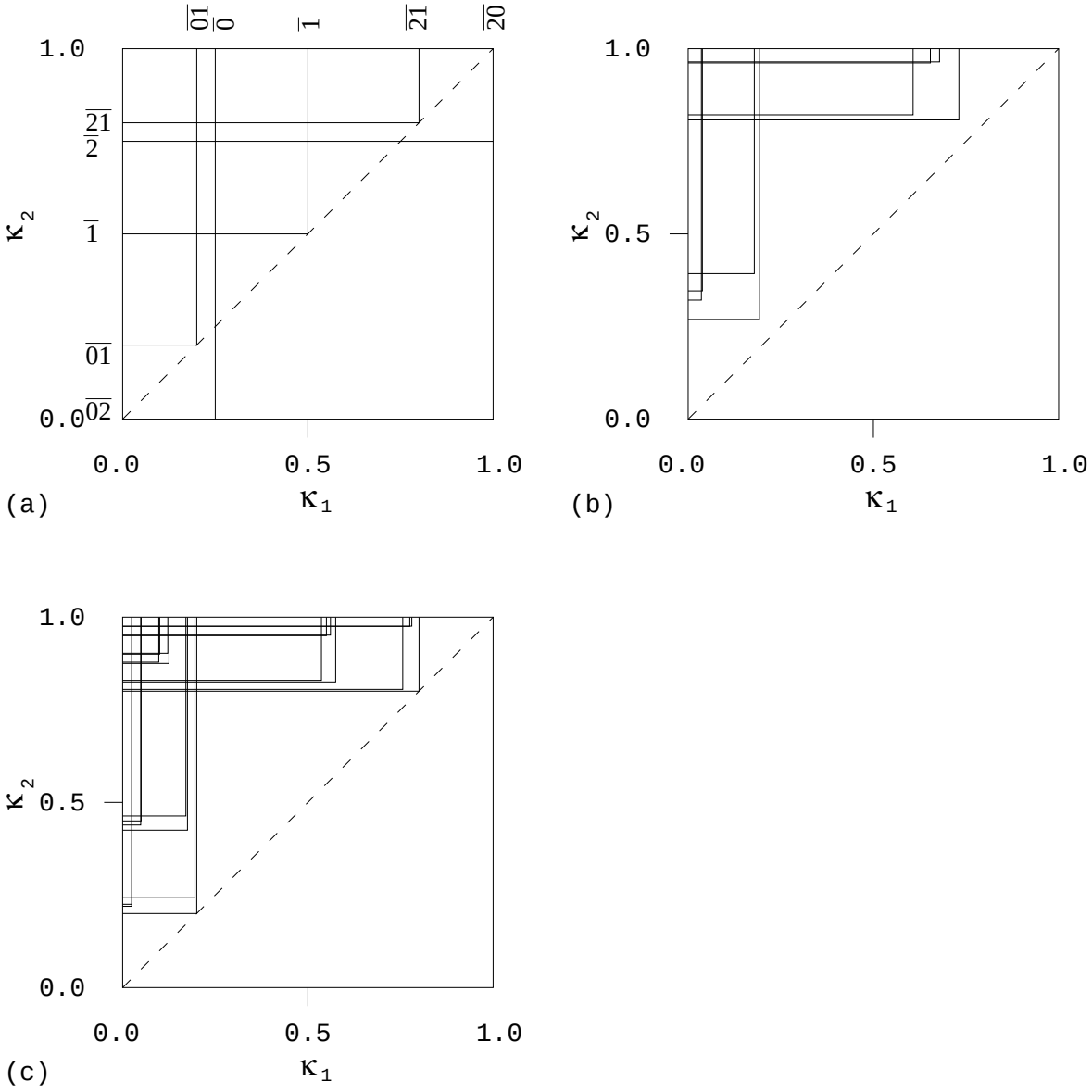

Figure 5: Symbolic parameter plane for the bimodal maps $-+-$ (a) period 1 and 2 orbits, (b) period 3 orbits, (c) period 4 orbits.

Figure 6: The bifurcation planes of fixed points in the trimodal map in the topological parameter space $(\kappa_1, \kappa_2, \kappa_3)$. The κ_2 axis is hidden behind the bifurcation planes.

Figure 7: The bifurcation planes of period 2 orbits in the trimodal map in the topological parameter space $(\kappa_1, \kappa_2, \kappa_3)$.

Figure 8: The bifurcation planes of period 3 orbits in the trimodal map in the topological parameter space $(\kappa_1, \kappa_2, \kappa_3)$, each plane labeled by the symbols for the period 3 orbit created at this parameter value.

Figure 9: The same as figure 8, but labeled with the swallowtail crossings rather than the individual period 3 orbits.

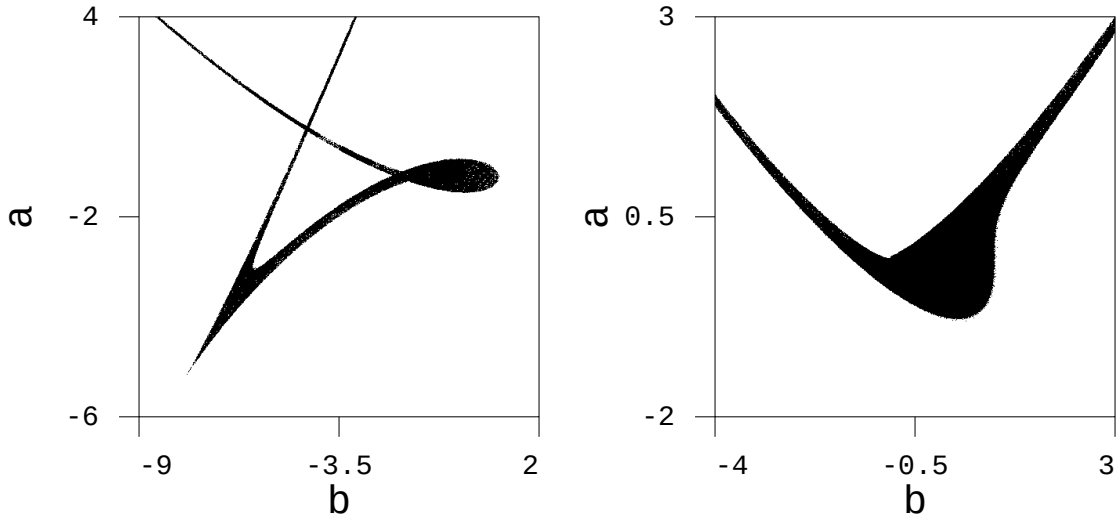

Figure 10: The area in parameter space (a, b) for the trimodal map where fixed points are stable, a) $c = -3$, b) $c = 0$.

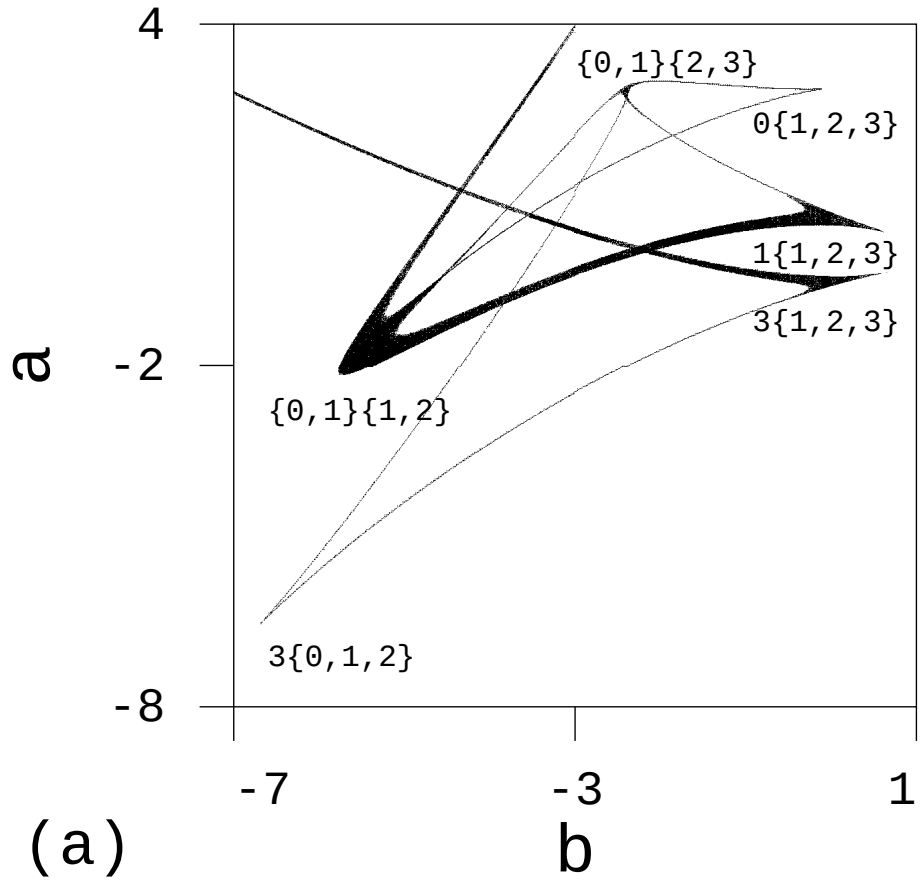

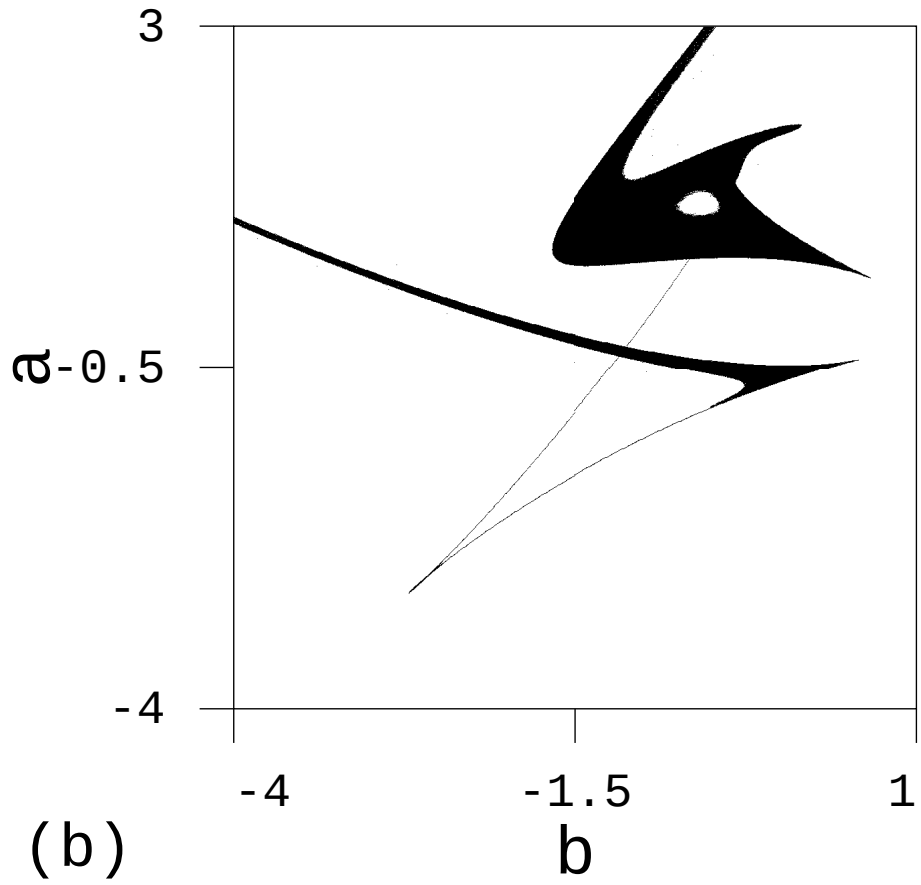

Figure 11: The area in parameter space (a, b) for the trimodal map where the period 2 orbits are stable, a) $c = -3$, b) $c = -2.2$.

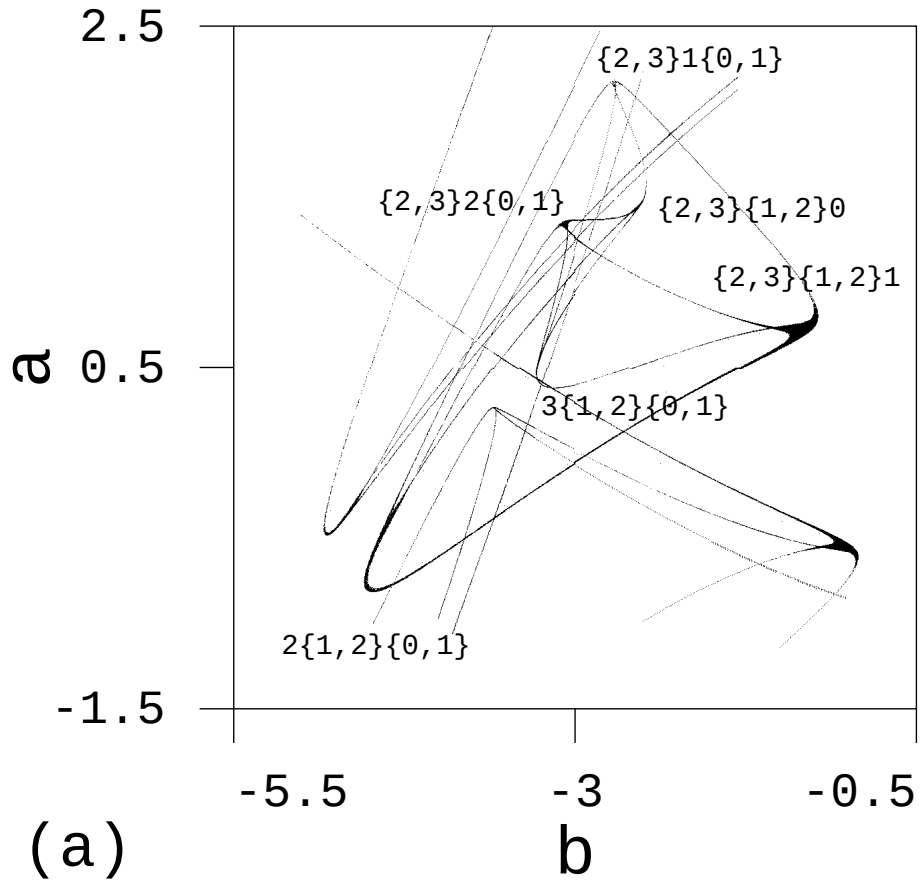

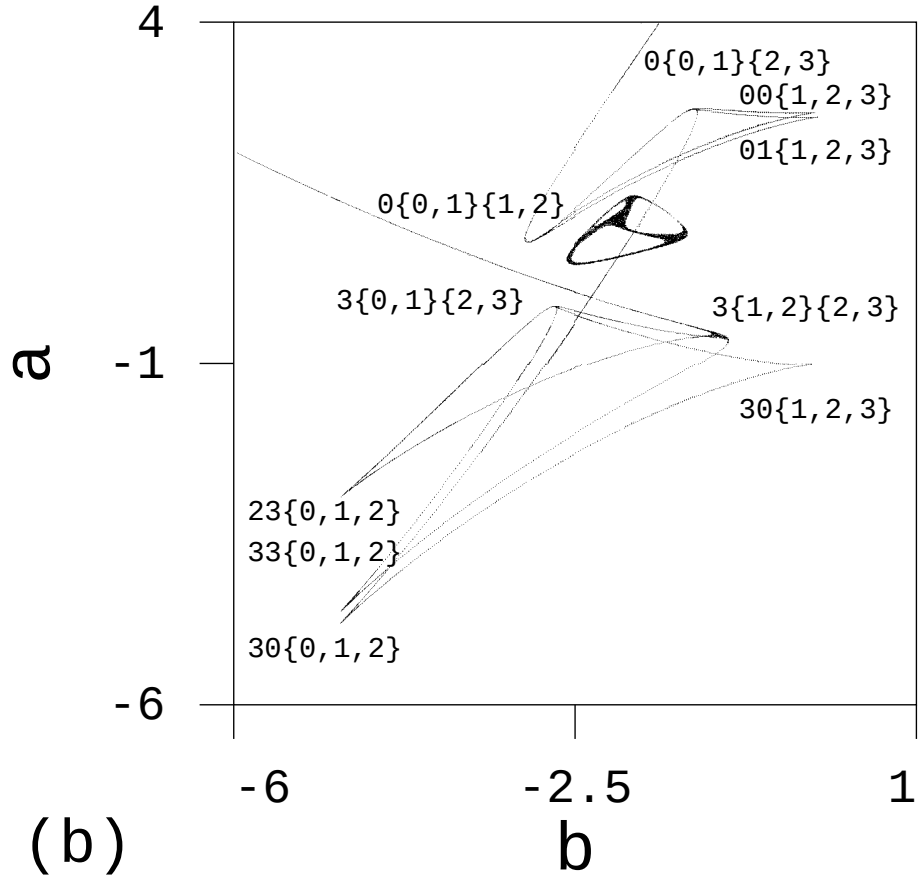

Figure 12: The area in parameter space (a, b) for the trimodal map where period 3 orbits are stable. (a) $c = -3$, (b) $c = -2.7$. The codimension two singularities are labeled using the symbolic description.

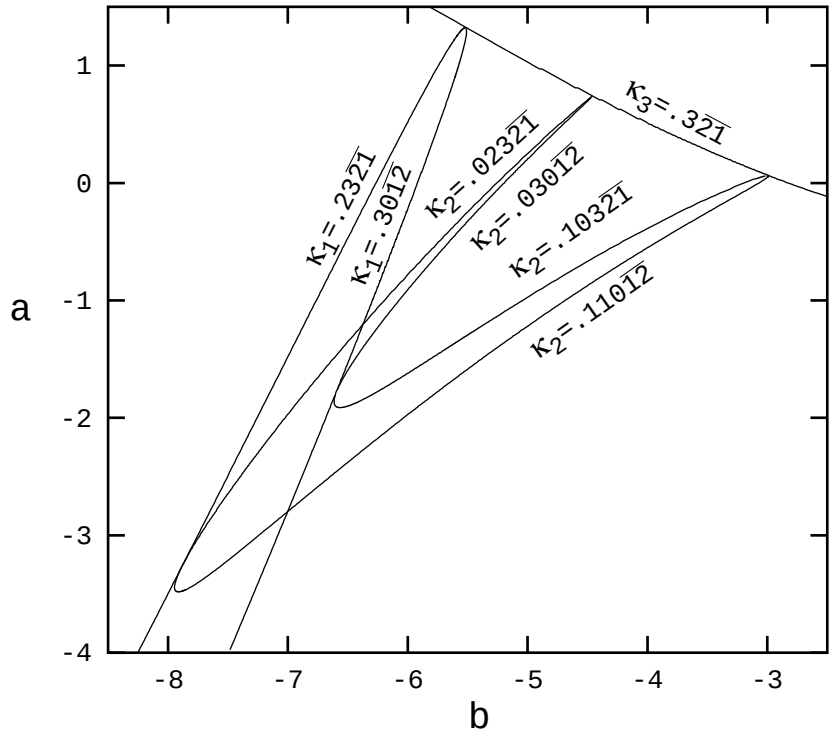

Figure 13: Bifurcation curves for homoclinic orbits in the parameter plane (a, b) for the trimodal map with $c = -3.5$.

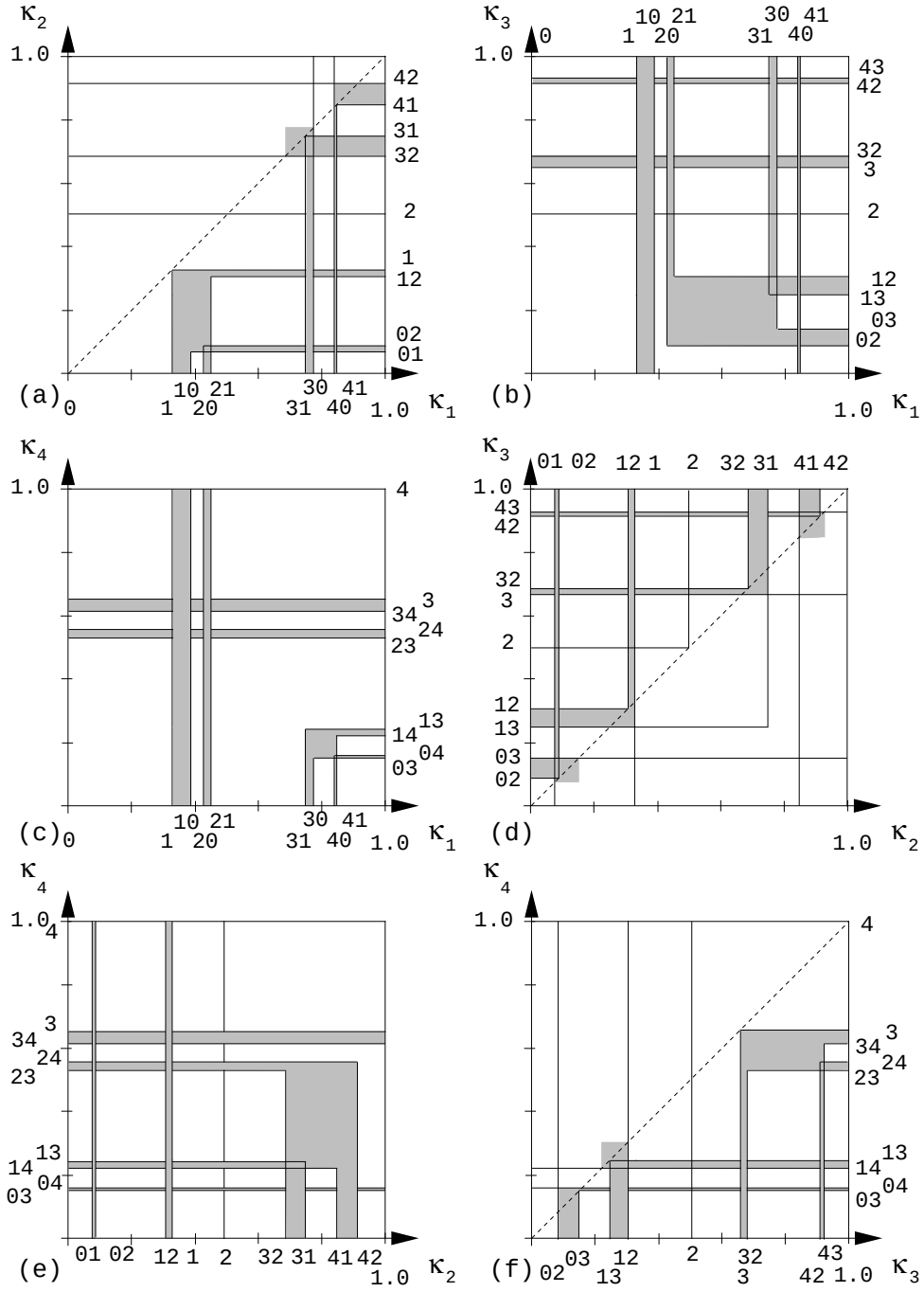

Figure 14: The six 2-dimensional symbolic bifurcation planes of period 1 and 2 orbits in the four modal map $+-+-+$.

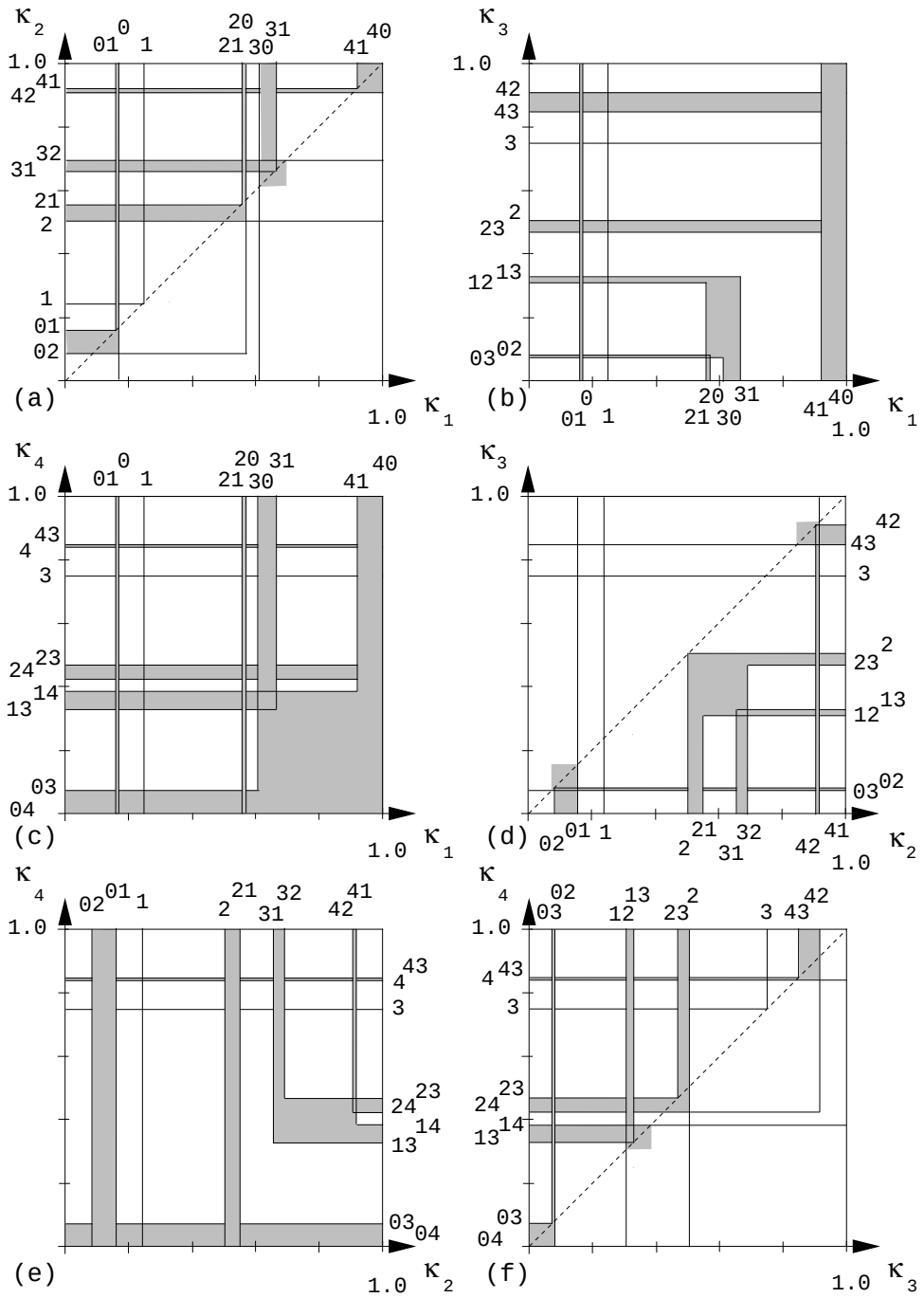

Figure 15: The six 2-dimensional symbolic bifurcation planes of period 1 and 2 orbits in the four modal map $-+-+-$.

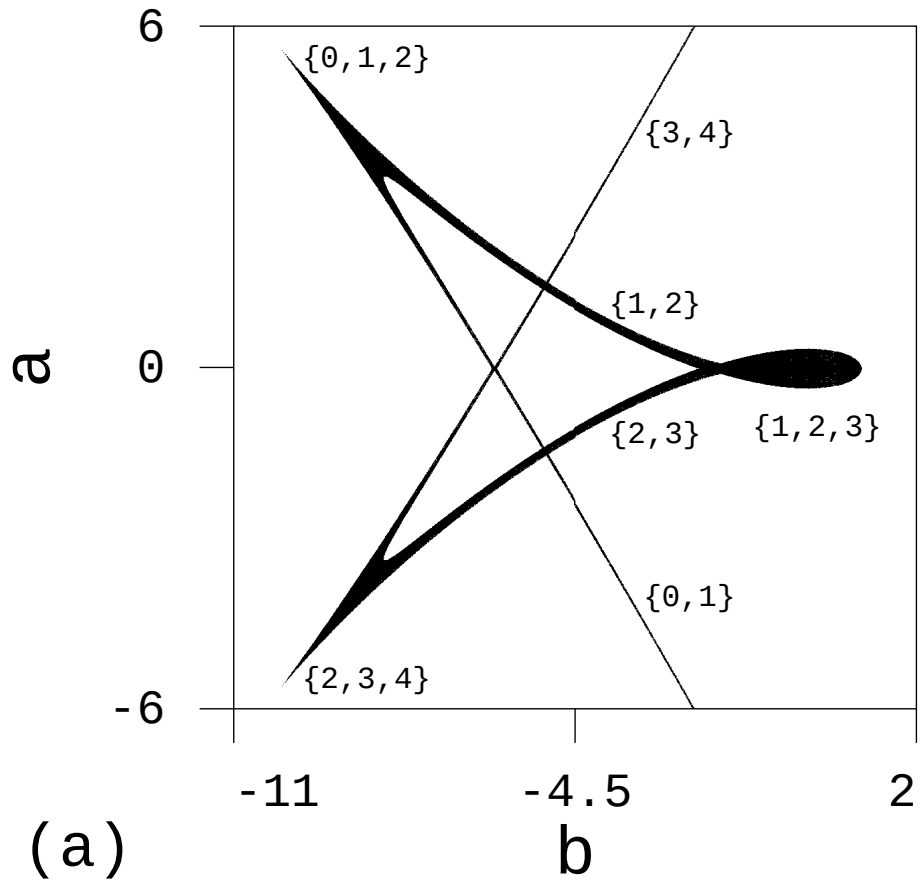

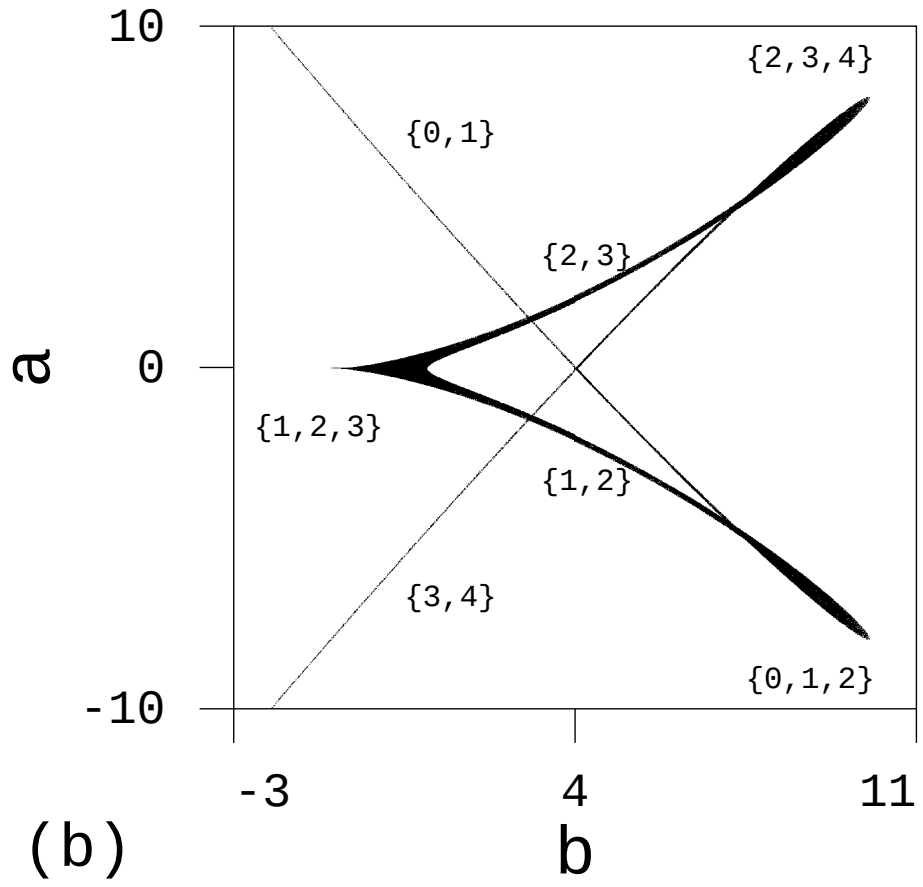

Figure 16: The area in parameter space (a, b) for the four modal maps (a) $+-+-+$, (b) $-+-+-$, where fixed points are stable, $d = 0$ and (a) $c = -4.5$,(b) $c = 4.5$.

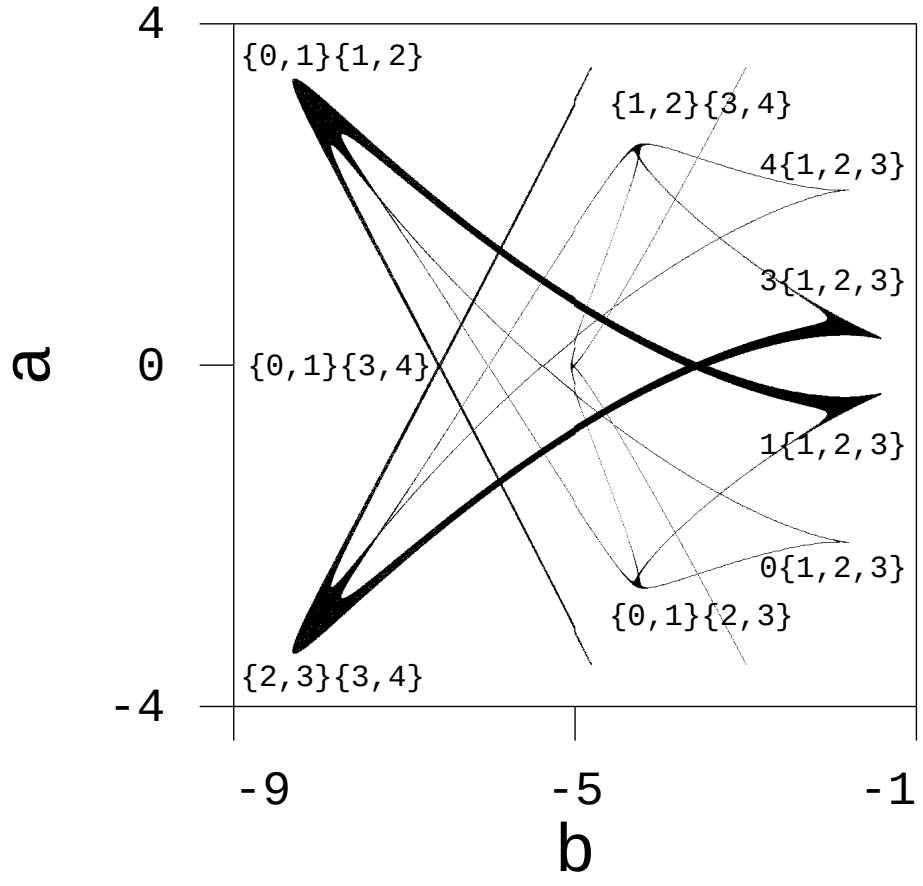

Figure 17: The area in the parameter plane (a, b) for the four modal map $+-+-+$ where period 2 orbits are stable, $d = 0$ and $c = -4.5$.

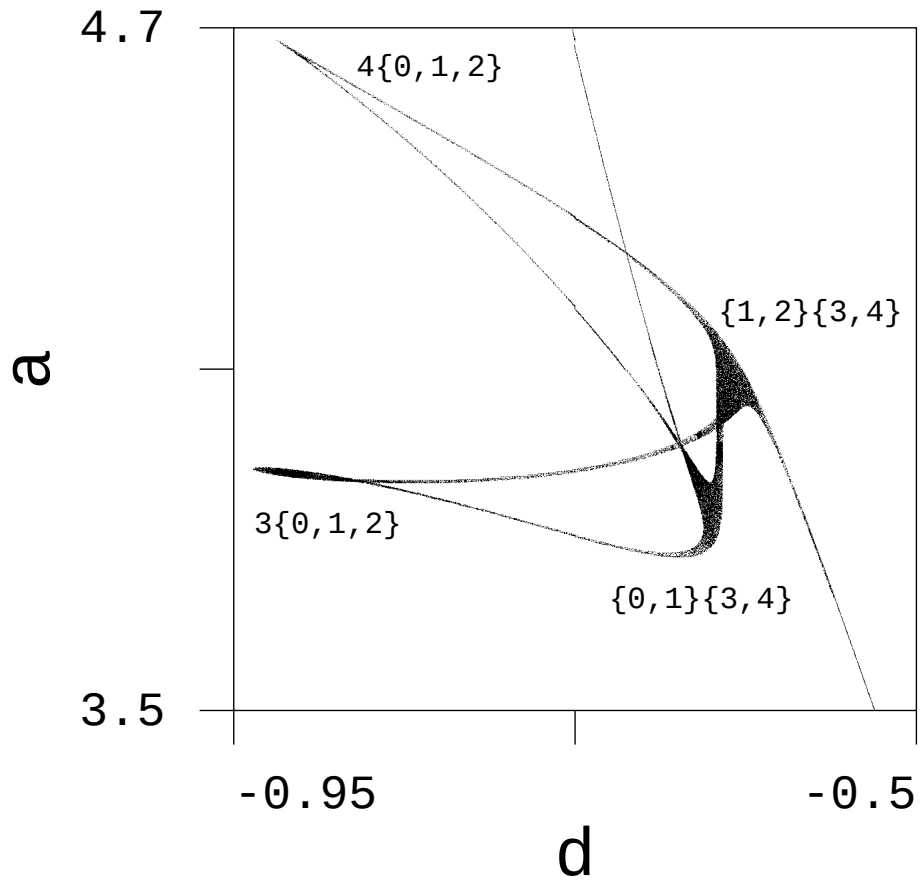

Figure 18: The area in the parameter plane (d, a) for the four modal map $+-+-+$ where period 2 orbits are stable, $b = -5$ and $c = -4.5$.

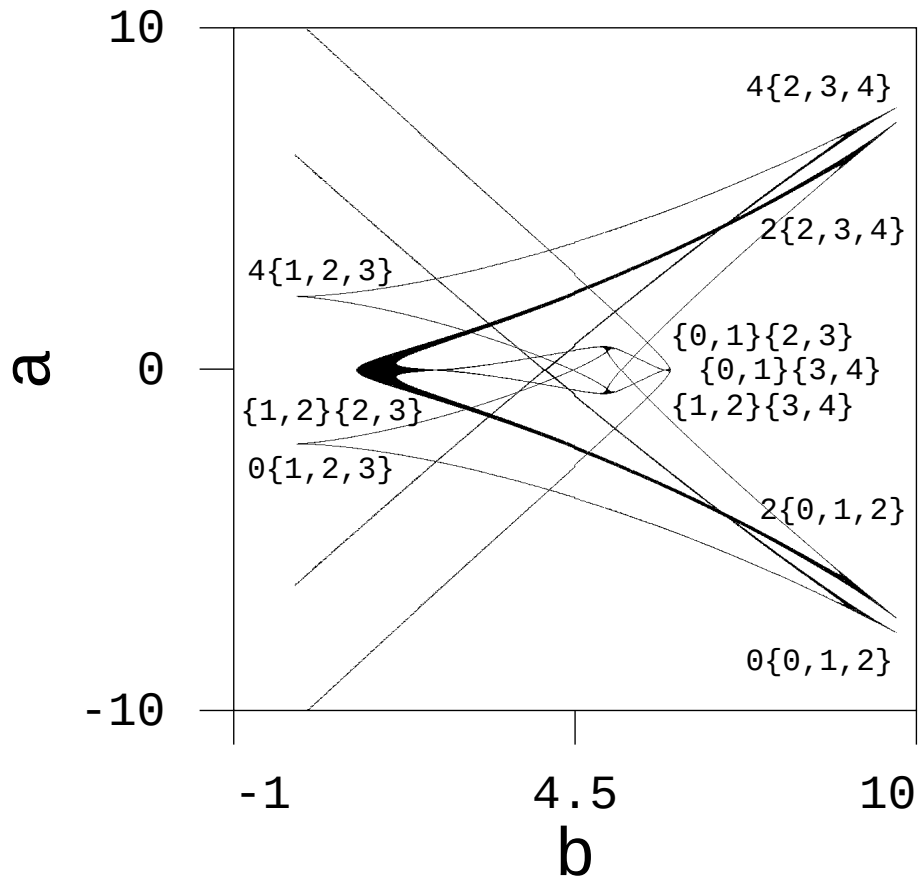

Figure 19: The area in the parameter plane (a, b) for the four modal map $-+-+-$, where period 2 orbits are stable, $d = 0$ and $c = 4.5$.

S	$\tau^{\max}$	S	$\tau^{\max}$
$\overline{0}$	$.\overline{0}$	$\overline{10111}$	$.\overline{11010} = 26/31$
$\overline{1}$	$.\overline{10} = 2/3$	$\overline{10110}$	$.\overline{1101100100} = 28/33$
$\overline{10}$	$.\overline{1100} = 4/5$	$\overline{10010}$	$.\overline{11100} = 28/31$
$\overline{101}$	$.\overline{110} = 6/7$	$\overline{10011}$	$.\overline{1110100010} = 10/11$
$\overline{100}$	$.\overline{111000} = 8/9$	$\overline{10001}$	$.\overline{11110} = 30/31$
$\overline{1011}$	$.\overline{11010010} = 14/17$	$\overline{10000}$	$.\overline{1111100000} = 32/33$
$\overline{1001}$	$.\overline{1110} = 14/15$		
$\overline{1000}$	$.\overline{11110000} = 16/17$		

Table 1: The symbolic values of the short periodic orbits of the unimodal map

S	$\tau_1^{\max}$	S	$\tau_2^{\min}$
$\overline{0}$	$.\overline{0}$		
$\overline{1}$	$.\overline{1} = 1/2$	$\overline{1}$	$.\overline{1} = 1/2$
		$\overline{2}$	$.\overline{2} = 1$
$\overline{10}$	$.\overline{1210} = 3/5$	$\overline{01}$	$.\overline{0121} = 1/5$
$\overline{20}$	$.\overline{20} = 3/4$	$\overline{02}$	$.\overline{02} = 1/4$
$\overline{21}$	$.\overline{2101} = 4/5$	$\overline{12}$	$.\overline{1012} = 2/5$
$\overline{101}$	$.\overline{121} = 8/13$	$\overline{011}$	$.\overline{011} = 2/13$
$\overline{100}$	$.\overline{122100} = 9/14$	$\overline{001}$	$.\overline{001221} = 1/14$
$\overline{200}$	$.\overline{200} = 9/13$	$\overline{002}$	$.\overline{002} = 1/13$
$\overline{201}$	$.\overline{201021} = 5/7$	$\overline{012}$	$.\overline{010212} = 1/7$
$\overline{211}$	$.\overline{211} = 11/13$	$\overline{121}$	$.\overline{101} = 5/13$
$\overline{210}$	$.\overline{212010} = 6/7$	$\overline{021}$	$.\overline{021201} = 2/7$
$\overline{220}$	$.\overline{220} = 12/13$	$\overline{022}$	$.\overline{022} = 4/13$
$\overline{221}$	$.\overline{221001} = 13/14$	$\overline{122}$	$.\overline{100122} = 5/14$
$\overline{1011}$	$.\overline{12111011} = 25/41$	$\overline{0111}$	$.\overline{01112111} = 7/41$
$\overline{1001}$	$.\overline{1221} = 13/20$	$\overline{0011}$	$.\overline{0011} = 1/20$
$\overline{1000}$	$.\overline{12221000} = 27/41$	$\overline{0001}$	$.\overline{00012221} = 1/41$
$\overline{2000}$	$.\overline{2000} = 27/40$	$\overline{0002}$	$.\overline{0002} = 1/40$
$\overline{2001}$	$.\overline{20010221} = 28/41$	$\overline{0012}$	$.\overline{00102212} = 2/41$
$\overline{2011}$	$.\overline{2011} = 29/40$	$\overline{0112}$	$.\overline{0112} = 7/40$
$\overline{2010}$	$.\overline{20120210} = 30/41$	$\overline{0102}$	$.\overline{01202102} = 3/41$
$\overline{2120}$	$.\overline{21020120} = 33/41$	$\overline{0212}$	$.\overline{02102012} = 11/41$
$\overline{2110}$	$.\overline{2110} = 33/40$	$\overline{0211}$	$.\overline{0211} = 11/40$
$\overline{2111}$	$.\overline{21110111} = 34/41$	$\overline{1211}$	$.\overline{10111211} = 16/41$
$\overline{2101}$	$.\overline{21} = 7/8$	$\overline{0121}$	$.\overline{01} = 1/8$
$\overline{2100}$	$.\overline{21220100} = 36/41$	$\overline{0021}$	$.\overline{00212201} = 4/41$
$\overline{2200}$	$.\overline{2200} = 9/10$	$\overline{0022}$	$.\overline{0022} = 1/10$
$\overline{2201}$	$.\overline{22010021} = 37/41$	$\overline{0122}$	$.\overline{01002122} = 5/41$
$\overline{2211}$	$.\overline{2211} = 19/20$	$\overline{1221}$	$.\overline{1001} = 7/20$
$\overline{2210}$	$.\overline{22120010} = 39/41$	$\overline{0221}$	$.\overline{02212001} = 13/41$
$\overline{2220}$	$.\overline{2220} = 39/40$	$\overline{0222}$	$.\overline{0222} = 13/40$

Table 2: The symbolic values of the short periodic orbits of the bimodal map $+-+$.

S	$\tau_1^{\min}$	S	$\tau_2^{\max}$
$\overline{0}$	$.\overline{02} = 1/4$		
$\overline{1}$	$.\overline{1} = 1/2$	$\overline{1}$	$.\overline{1} = 1/2$
		$\overline{2}$	$.\overline{20} = 3/4$
$\overline{01}$	$.\overline{0121} = 1/5$	$\overline{01}$	$.\overline{0121} = 1/5$
$\overline{21}$	$.\overline{2101} = 4/5$	$\overline{21}$	$.\overline{2101} = 4/5$
$\overline{20}$	$.\overline{2} = 1$	$\overline{02}$	$.\overline{0} = 0$
$\overline{020}$	$.\overline{000222} = 1/28$	$\overline{002}$	$.\overline{022200} = 9/28$
$\overline{021}$	$.\overline{001} = 1/26$	$\overline{102}$	$.\overline{100} = 9/26$
$\overline{011}$	$.\overline{011211} = 5/28$	$\overline{101}$	$.\overline{101121} = 11/28$
$\overline{010}$	$.\overline{012} = 5/26$	$\overline{001}$	$.\overline{021} = 7/26$
$\overline{121}$	$.\overline{121101} = 17/28$	$\overline{211}$	$.\overline{211011} = 23/28$
$\overline{120}$	$.\overline{122} = 17/26$	$\overline{201}$	$.\overline{221} = 25/26$
$\overline{220}$	$.\overline{200022} = 19/28$	$\overline{202}$	$.\overline{222000} = 27/28$
$\overline{221}$	$.\overline{201} = 19/26$	$\overline{212}$	$.\overline{210} = 21/26$
$\overline{0201}$	$.\overline{00012221} = 1/41$	$\overline{0102}$	$.\overline{01222100} = 9/41$
$\overline{0200}$	$.\overline{0002} = 1/40$	$\overline{0002}$	$.\overline{0200} = 9/40$
$\overline{0210}$	$.\overline{00102212} = 2/41$	$\overline{1002}$	$.\overline{10221200} = 18/41$
$\overline{0211}$	$.\overline{0011} = 1/20$	$\overline{1102}$	$.\overline{1100} = 9/20$
$\overline{0221}$	$.\overline{00212201} = 4/41$	$\overline{2102}$	$.\overline{21220100} = 36/41$
$\overline{0220}$	$.\overline{0022} = 1/10$	$\overline{2002}$	$.\overline{2200} = 9/10$
$\overline{0120}$	$.\overline{01002122} = 5/41$	$\overline{2001}$	$.\overline{22010021} = 37/41$
$\overline{0121}$	$.\overline{01} = 1/8$	$\overline{2101}$	$.\overline{21} = 7/8$
$\overline{0111}$	$.\overline{01112111} = 7/41$	$\overline{1101}$	$.\overline{11011121} = 19/41$
$\overline{0110}$	$.\overline{0112} = 7/40$	$\overline{1001}$	$.\overline{1021} = 17/40$
$\overline{0100}$	$.\overline{01202102} = 8/41$	$\overline{0001}$	$.\overline{02012021} = 10/41$
$\overline{1121}$	$.\overline{11211101} = 22/41$	$\overline{2111}$	$.\overline{21110111} = 34/41$
$\overline{1120}$	$.\overline{1122} = 11/20$	$\overline{2011}$	$.\overline{2211} = 19/20$
$\overline{1220}$	$.\overline{12001022} = 23/41$	$\overline{2012}$	$.\overline{22120010} = 39/31$
$\overline{1221}$	$.\overline{1201} = 23/40$	$\overline{2112}$	$.\overline{2110} = 33/40$
$\overline{2221}$	$.\overline{20210201} = 31/41$	$\overline{2122}$	$.\overline{21020120} = 33/41$
$\overline{2220}$	$.\overline{2022} = 31/40$	$\overline{2022}$	$.\overline{2220} = 39/40$
$\overline{2120}$	$.\overline{21000122} = 32/41$	$\overline{2021}$	$.\overline{22210001} = 40/41$

Table 3: The symbolic values of the short periodic orbits of the bimodal map $-+-$.

S	$\tau_1^{\max}$	S	$\tau_2^{\min}$	S	$\tau_3^{\max}$
				$\overline{3}$	$.\overline{30}$
		$\overline{2}$	$.\overline{2}$	$\overline{2}$	$.\overline{2}$
$\overline{1}$	$.\overline{12}$	$\overline{1}$	$.\overline{12}$		
$\overline{0}$	$.\overline{0}$				
$\overline{30}$	$.\overline{3300}$			$\overline{03}$	$.\overline{0330}$
$\overline{31}$	$.\overline{32}$	$\overline{31}$	$.\overline{32}$	$\overline{13}$	$.\overline{10}$
		$\overline{32}$	$.\overline{3102}$	$\overline{32}$	$.\overline{3102}$
$\overline{21}$	$.\overline{2112}$	$\overline{12}$	$.\overline{1122}$	$\overline{12}$	$.\overline{1122}$
$\overline{20}$	$.\overline{20}$	$\overline{02}$	$.\overline{02}$	$\overline{02}$	$.\overline{02}$
$\overline{10}$	$.\overline{1320}$	$\overline{01}$	$.\overline{0132}$		

S	$\tau_1^{\max}$	S	$\tau_2^{\min}$	S	$\tau_3^{\max}$
$\overline{300}$	$.\overline{333000}$			$\overline{003}$	$.\overline{003330}$
$\overline{301}$	$.\overline{332}$	$\overline{301}$	$.\overline{332}$	$\overline{013}$	$.\overline{010}$
$\overline{230}$	$.\overline{233100}$	$\overline{302}$	$.\overline{331002}$	$\overline{302}$	$.\overline{331002}$
$\overline{330}$	$.\overline{300}$			$\overline{303}$	$.\overline{330}$
$\overline{331}$	$.\overline{301032}$	$\overline{331}$	$.\overline{301032}$	$\overline{313}$	$.\overline{323010}$
$\overline{231}$	$.\overline{232}$	$\overline{231}$	$.\overline{232}$	$\overline{312}$	$.\overline{322}$
$\overline{311}$	$.\overline{321012}$	$\overline{131}$	$.\overline{101232}$	$\overline{113}$	$.\overline{123210}$
$\overline{310}$	$.\overline{320}$	$\overline{031}$	$.\overline{032}$	$\overline{103}$	$.\overline{130}$
$\overline{320}$	$.\overline{313020}$	$\overline{032}$	$.\overline{031302}$	$\overline{203}$	$.\overline{2031130}$
$\overline{321}$	$.\overline{312}$	$\overline{132}$	$.\overline{102}$	$\overline{213}$	$.\overline{210}$
		$\overline{232}$	$.\overline{231102}$	$\overline{322}$	$.\overline{311022}$
		$\overline{332}$	$.\overline{302}$	$\overline{323}$	$.\overline{310}$
$\overline{221}$	$.\overline{221112}$	$\overline{122}$	$.\overline{111222}$	$\overline{212}$	$.\overline{211122}$
$\overline{220}$	$.\overline{220}$	$\overline{022}$	$.\overline{022}$	$\overline{202}$	$.\overline{202}$
$\overline{210}$	$.\overline{213120}$	$\overline{021}$	$.\overline{021312}$	$\overline{102}$	$.\overline{131202}$
$\overline{211}$	$.\overline{212}$	$\overline{121}$	$.\overline{112}$	$\overline{112}$	$.\overline{122}$
$\overline{201}$	$.\overline{201132}$	$\overline{012}$	$.\overline{011322}$	$\overline{012}$	$.\overline{011322}$
$\overline{200}$	$.\overline{200}$	$\overline{002}$	$.\overline{002}$	$\overline{002}$	$.\overline{002}$
$\overline{100}$	$.\overline{133200}$	$\overline{001}$	$.\overline{0011332}$		
$\overline{101}$	$.\overline{132}$	$\overline{011}$	$.\overline{012}$		

Table 4: The fixed points, period 2 and period 3 orbits in the trimodal map with the kneading values giving the topological bifurcation diagrams in figures 6, 7, 8 and 9.

S	$\tau_1^{\max}$	S	$\tau_2^{\min}$	S	$\tau_3^{\max}$	S	$\tau_4^{\min}$
						$\overline{4}$	$.\overline{4}$
				$\overline{3}$	$.\overline{31}$	$\overline{3}$	$.\overline{31}$
		$\overline{2}$	$.\overline{2}$	$\overline{2}$	$.\overline{2}$		
$\overline{1}$	$.\overline{13}$	$\overline{1}$	$.\overline{13}$				
$\overline{0}$	$.\overline{0}$						
				$\overline{43}$	$.\overline{4301}$	$\overline{34}$	$.\overline{3014}$
		$\overline{42}$	$.\overline{42}$	$\overline{42}$	$.\overline{42}$	$\overline{24}$	$.\overline{24}$
$\overline{41}$	$.\overline{4103}$	$\overline{41}$	$.\overline{4103}$			$\overline{14}$	$.\overline{1034}$
$\overline{40}$	$.\overline{40}$					$\overline{04}$	$.\overline{04}$
$\overline{30}$	$.\overline{3410}$			$\overline{03}$	$.\overline{0341}$	$\overline{03}$	$.\overline{0341}$
$\overline{31}$	$.\overline{3}$	$\overline{31}$	$.\overline{3}$	$\overline{13}$	$.\overline{1}$	$\overline{13}$	$.\overline{1}$
		$\overline{32}$	$.\overline{3212}$	$\overline{32}$	$.\overline{3212}$	$\overline{23}$	$.\overline{2321}$
$\overline{21}$	$.\overline{2123}$	$\overline{12}$	$.\overline{1232}$	$\overline{12}$	$.\overline{1232}$		
$\overline{20}$	$.\overline{20}$	$\overline{02}$	$.\overline{02}$	$\overline{02}$	$.\overline{02}$		
$\overline{10}$	$.\overline{1430}$	$\overline{01}$	$.\overline{0143}$				

Table 5: The fixed points and period 2 orbits in the four-modal map $+-+-+$ with the kneading values giving the topological bifurcation diagrams in figure 14.

S	$\tau_1^{\max}$	S	$\tau_2^{\min}$	S	$\tau_3^{\max}$	S	$\tau_4^{\min}$
				$\overline{443}$	$.\overline{443001}$	$\overline{344}$	$.\overline{300144}$
		$\overline{442}$	$.\overline{442}$	$\overline{442}$	$.\overline{442}$	$\overline{244}$	$.\overline{244}$
$\overline{441}$	$.\overline{441003}$	$\overline{441}$	$.\overline{441003}$			$\overline{144}$	$.\overline{100344}$
$\overline{440}$	$.\overline{440}$					$\overline{044}$	$.\overline{044}$
				$\overline{433}$	$.\overline{431}$	$\overline{343}$	$.\overline{301}$
		$\overline{432}$	$.\overline{432012}$	$\overline{432}$	$.\overline{432012}$	$\overline{324}$	$.\overline{320124}$
$\overline{431}$	$.\overline{433}$	$\overline{431}$	$.\overline{433}$	$\overline{143}$	$.\overline{101}$	$\overline{143}$	$.\overline{101}$
$\overline{430}$	$.\overline{434010}$			$\overline{043}$	$.\overline{043401}$	$\overline{043}$	$.\overline{043401}$
		$\overline{342}$	$.\overline{302142}$	$\overline{423}$	$.\overline{423021}$	$\overline{234}$	$.\overline{230214}$
		$\overline{242}$	$.\overline{242}$	$\overline{422}$	$.\overline{422}$	$\overline{224}$	$.\overline{224}$
$\overline{421}$	$.\overline{421023}$	$\overline{142}$	$.\overline{102342}$	$\overline{142}$	$.\overline{102342}$	$\overline{214}$	$.\overline{210234}$
$\overline{420}$	$.\overline{420}$	$\overline{042}$	$.\overline{042}$	$\overline{042}$	$.\overline{042}$	$\overline{204}$	$.\overline{204}$
$\overline{341}$	$.\overline{303}$	$\overline{341}$	$.\overline{303}$	$\overline{413}$	$.\overline{411}$	$\overline{134}$	$.\overline{114}$
$\overline{241}$	$.\overline{241203}$	$\overline{241}$	$.\overline{241203}$	$\overline{412}$	$.\overline{412032}$	$\overline{124}$	$.\overline{120324}$
$\overline{411}$	$\overline{413}$	$\overline{141}$	$.\overline{103}$			$\overline{114}$	$.\overline{134}$
$\overline{410}$	$.\overline{414014}$	$\overline{041}$	$.\overline{041401}$			$\overline{104}$	$.\overline{140304}$
$\overline{340}$	$.\overline{304140}$			$\overline{403}$	$.\overline{403041}$	$\overline{034}$	$.\overline{030414}$
$\overline{240}$	$.\overline{240}$	$\overline{402}$	$.\overline{402}$	$\overline{402}$	$.\overline{402}$	$\overline{024}$	$.\overline{024}$
$\overline{401}$	$.\overline{401043}$	$\overline{401}$	$.\overline{401043}$			$\overline{014}$	$.\overline{010434}$
$\overline{400}$	$.\overline{400}$					$\overline{004}$	$.\overline{004}$
		$\overline{332}$	$.\overline{312}$	$\overline{323}$	$.\overline{321}$	$\overline{233}$	$.\overline{231}$
$\overline{331}$	$.\overline{311133}$	$\overline{331}$	$.\overline{311133}$	$\overline{313}$	$.\overline{333111}$	$\overline{133}$	$.\overline{113331}$
$\overline{330}$	$.\overline{310}$			$\overline{303}$	$.\overline{341}$	$\overline{033}$	$.\overline{031}$
		$\overline{232}$	$.\overline{232212}$	$\overline{322}$	$.\overline{322122}$	$\overline{223}$	$.\overline{223221}$
$\overline{321}$	$.\overline{323}$	$\overline{132}$	$.\overline{112}$	$\overline{213}$	$.\overline{211}$	$\overline{213}$	$.\overline{211}$
$\overline{320}$	$.\overline{324120}$	$\overline{032}$	$.\overline{032412}$	$\overline{203}$	$.\overline{203241}$	$\overline{203}$	$.\overline{203241}$
$\overline{231}$	$.\overline{233}$	$\overline{231}$	$.\overline{233}$	$\overline{312}$	$.\overline{332}$	$\overline{123}$	$.\overline{121}$
$\overline{311}$	$.\overline{331113}$	$\overline{131}$	$.\overline{111333}$	$\overline{113}$	$.\overline{133311}$	$\overline{113}$	$.\overline{133311}$
$\overline{310}$	$.\overline{330}$	$\overline{031}$	$.\overline{033}$	$\overline{103}$	$.\overline{141}$	$\overline{103}$	$.\overline{141}$
$\overline{230}$	$.\overline{234210}$	$\overline{302}$	$.\overline{342102}$	$\overline{302}$	$.\overline{342102}$	$\overline{023}$	$.\overline{023421}$
$\overline{301}$	$.\overline{343}$	$\overline{301}$	$.\overline{343}$	$\overline{013}$	$.\overline{011}$	$\overline{013}$	$.\overline{011}$
$\overline{300}$	$.\overline{344100}$			$\overline{003}$	$.\overline{003441}$	$\overline{003}$	$.\overline{003441}$
$\overline{221}$	$.\overline{221223}$	$\overline{122}$	$.\overline{122322}$	$\overline{212}$	$.\overline{212232}$		
$\overline{220}$	$.\overline{220}$	$\overline{022}$	$.\overline{022}$	$\overline{202}$	$.\overline{202}$		
$\overline{211}$	$.\overline{213}$	$\overline{121}$	$.\overline{123}$	$\overline{112}$	$.\overline{132}$		
$\overline{210}$	$.\overline{214230}$	$\overline{021}$	$.\overline{021423}$	$\overline{102}$	$.\overline{142302}$		
$\overline{201}$	$.\overline{201243}$	$\overline{012}$	$.\overline{012432}$	$\overline{012}$	$.\overline{012432}$		
$\overline{200}$	$.\overline{200}$	$\overline{002}$	$.\overline{002}$	$\overline{002}$	$.\overline{002}$		
$\overline{101}$	$.\overline{143}$	$\overline{011}$	$.\overline{013}$				
$\overline{100}$	$.\overline{144300}$	$\overline{001}$	$.\overline{001443}$				

Table 6: The period 3 orbits in the four-modal map $+-+-+$ with the kneading values.

S	$\tau_1^{\min}$	S	$\tau_2^{\max}$	S	$\tau_3^{\min}$	S	$\tau_4^{\max}$
						$\overline{4}$	$.\overline{40}$
				$\overline{3}$	$.\overline{3}$	$\overline{3}$	$.\overline{3}$
		$\overline{2}$	$.\overline{2}$	$\overline{2}$	$.\overline{2}$		
$\overline{1}$	$.\overline{1}$	$\overline{1}$	$.\overline{1}$				
$\overline{0}$	$.\overline{04}$						
				$\overline{43}$	$.\overline{4103}$	$\overline{43}$	$.\overline{4103}$
		$\overline{42}$	$.\overline{42}$	$\overline{42}$	$.\overline{42}$	$\overline{24}$	$.\overline{20}$
$\overline{41}$	$.\overline{4301}$	$\overline{41}$	$.\overline{4301}$			$\overline{14}$	$.\overline{1430}$
$\overline{40}$	$.\overline{4}$					$\overline{04}$	$.\overline{0}$
$\overline{30}$	$.\overline{3014}$			$\overline{03}$	$.\overline{0143}$	$\overline{03}$	$.\overline{0143}$
$\overline{31}$	$.\overline{31}$	$\overline{31}$	$.\overline{31}$	$\overline{13}$	$.\overline{13}$	$\overline{13}$	$.\overline{13}$
		$\overline{32}$	$.\overline{3212}$	$\overline{23}$	$.\overline{2123}$	$\overline{23}$	$.\overline{2123}$
$\overline{21}$	$.\overline{2321}$	$\overline{21}$	$.\overline{2321}$	$\overline{12}$	$.\overline{1232}$		
$\overline{20}$	$.\overline{24}$	$\overline{02}$	$.\overline{02}$	$\overline{02}$	$.\overline{02}$		
$\overline{01}$	$.\overline{0341}$	$\overline{01}$	$.\overline{0341}$				

Table 7: The fixed points, period 2 (and period 3) orbits in the four-modal map $-+-+-$ with the kneading values giving the topological bifurcation diagrams in figure 15.

S	$\tau_1^{\min}$	S	$\tau_2^{\max}$	S	$\tau_3^{\min}$	S	$\tau_4^{\max}$
				$\overline{443}$	$.\overline{403}$	$\overline{434}$	$.\overline{410}$
		$\overline{442}$	$.\overline{402042}$	$\overline{442}$	$.\overline{402042}$	$\overline{424}$	$.\overline{424020}$
$\overline{441}$	$.\overline{401}$	$\overline{441}$	$.\overline{401}$			$\overline{414}$	$.\overline{430}$
$\overline{440}$	$.\overline{400044}$					$\overline{404}$	$.\overline{444000}$
				$\overline{343}$	$.\overline{341103}$	$\overline{433}$	$.\overline{411033}$
		$\overline{432}$	$.\overline{412}$	$\overline{243}$	$.\overline{203}$	$\overline{324}$	$.\overline{320}$
$\overline{431}$	$.\overline{413031}$	$\overline{431}$	$.\overline{413031}$	$\overline{143}$	$.\overline{141303}$	$\overline{314}$	$.\overline{314130}$
$\overline{430}$	$.\overline{414}$			$\overline{043}$	$.\overline{003}$	$\overline{304}$	$.\overline{300}$
		$\overline{342}$	$.\overline{342}$	$\overline{342}$	$.\overline{342}$	$\overline{423}$	$.\overline{423}$
		$\overline{422}$	$.\overline{422022}$	$\overline{242}$	$.\overline{202242}$	$\overline{224}$	$.\overline{224220}$
$\overline{421}$	$.\overline{421}$	$\overline{421}$	$.\overline{421}$	$\overline{142}$	$.\overline{142}$	$\overline{214}$	$.\overline{230}$
$\overline{420}$	$.\overline{420024}$	$\overline{042}$	$.\overline{002442}$	$\overline{042}$	$.\overline{002442}$	$\overline{204}$	$.\overline{244200}$
$\overline{341}$	$.\overline{343101}$	$\overline{341}$	$.\overline{343101}$	$\overline{413}$	$.\overline{431013}$	$\overline{413}$	$.\overline{431013}$
$\overline{241}$	$.\overline{201}$	$\overline{412}$	$.\overline{432}$	$\overline{412}$	$.\overline{432}$	$\overline{124}$	$.\overline{120}$
$\overline{141}$	$\overline{143301}$	$\overline{411}$	$.\overline{433011}$			$\overline{114}$	$.\overline{114330}$
$\overline{041}$	$.\overline{001}$	$\overline{041}$	$.\overline{001}$			$\overline{104}$	$.\overline{100}$
$\overline{340}$	$.\overline{344}$			$\overline{403}$	$.\overline{443}$	$\overline{403}$	$.\overline{443}$
$\overline{240}$	$.\overline{200244}$	$\overline{402}$	$.\overline{442002}$	$\overline{402}$	$.\overline{442002}$	$\overline{024}$	$.\overline{024420}$
$\overline{140}$	$.\overline{144}$	$\overline{401}$	$.\overline{441}$			$\overline{014}$	$.\overline{030}$
$\overline{040}$	$.\overline{000444}$					$\overline{004}$	$.\overline{044400}$
		$\overline{332}$	$.\overline{332112}$	$\overline{233}$	$.\overline{211233}$	$\overline{323}$	$.\overline{321123}$
$\overline{331}$	$.\overline{331}$	$\overline{331}$	$.\overline{331}$	$\overline{133}$	$.\overline{311}$	$\overline{313}$	$.\overline{313}$
$\overline{330}$	$.\overline{330114}$			$\overline{033}$	$.\overline{011433}$	$\overline{303}$	$.\overline{301143}$
		$\overline{322}$	$.\overline{322}$	$\overline{232}$	$.\overline{212}$	$\overline{223}$	$.\overline{223}$
$\overline{321}$	$.\overline{323121}$	$\overline{321}$	$.\overline{323121}$	$\overline{132}$	$.\overline{132312}$	$\overline{213}$	$.\overline{231213}$
$\overline{320}$	$.\overline{324}$	$\overline{032}$	$.\overline{012}$	$\overline{032}$	$.\overline{012}$	$\overline{203}$	$.\overline{243}$
$\overline{231}$	$.\overline{213231}$	$\overline{312}$	$.\overline{312132}$	$\overline{123}$	$.\overline{121323}$	$\overline{123}$	$.\overline{121323}$
$\overline{131}$	$.\overline{131}$	$\overline{311}$	$.\overline{311}$	$\overline{113}$	$.\overline{113}$	$\overline{113}$	$.\overline{113}$
$\overline{031}$	$.\overline{013431}$	$\overline{031}$	$.\overline{013431}$	$\overline{103}$	$.\overline{101343}$	$\overline{103}$	$.\overline{101343}$
$\overline{230}$	$.\overline{214}$	$\overline{302}$	$.\overline{302}$	$\overline{023}$	$.\overline{023}$	$\overline{023}$	$.\overline{023}$
$\overline{130}$	$.130314$	$\overline{301}$	$.303141$	$\overline{013}$	$.\overline{031413}$	$\overline{013}$	$.\overline{031413}$
$\overline{030}$	$.\overline{014}$			$\overline{003}$	$.\overline{043}$	$\overline{003}$	$.\overline{043}$
$\overline{221}$	$.\overline{221}$	$\overline{212}$	$.\overline{232}$	$\overline{122}$	$.\overline{122}$		
$\overline{220}$	$.220224$	$\overline{202}$	$.\overline{242202}$	$\overline{022}$	$.\overline{022422}$		
$\overline{121}$	$.\overline{123321}$	$\overline{211}$	$.\overline{233211}$	$\overline{112}$	$.\overline{112332}$		
$\overline{021}$	$.\overline{021}$	$\overline{102}$	$.\overline{102}$	$\overline{102}$	$.\overline{102}$		
$\overline{120}$	$.\overline{124}$	$\overline{201}$	$.\overline{241}$	$\overline{012}$	$.\overline{032}$		
$\overline{020}$	$.\overline{020424}$	$\overline{002}$	$.\overline{042402}$	$\overline{002}$	$.\overline{042402}$		
$\overline{011}$	$.\overline{033411}$	$\overline{101}$	$.\overline{103341}$				
$\overline{010}$	$.\overline{034}$	$\overline{001}$	$.\overline{041}$				

Table 8: The period 3 orbits in the four-modal map $-+-+-$ with the kneading values.